AD-A143 647 THE CALCULATION OF THE RADAR VERTICAL COVERAGE DIAGRAM 1/1
(U) ROYAL AUSTRALIAN NAVY RESEARCH LAB EDGECLIFF
M R BATTAGLIA MAY 84 RANRL-T/NOTE(EXT)-1/84

UNCLASSIFIED F/G 17/9 NL

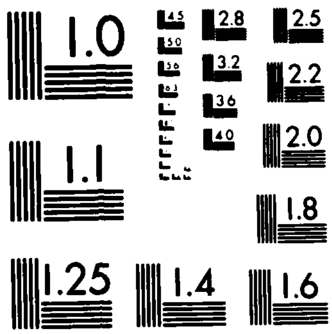

MICROCOPY RESOLUTION TEST CHART
NATIONAL BUREAU OF STANDARDS-1963-A

RANRL T/Note (Ext)-1/84 AR Number: AR003-419

DEPARTMENT OF DEFENCE

DEFENCE SCIENCE AND TECHNOLOGY ORGANISATION

R.A.N. RESEARCH LABORATORY

EDGECLIFF, N.S.W.

RANRL TECHNICAL NOTE

(External) No 1/84

THE CALCULATION OF THE RADAR VERTICAL COVERAGE DIAGRAM

M.R.BATTAGLIA

UNCLASSIFIED

DEPARTMENT OF DEFENCE

R.A.N. RESEARCH LABORATORY

RANRL TECHNICAL NOTE (EXTERNAL) No 1/84

THE CALCULATION OF THE RADAR VERTICAL COVERAGE DIAGRAM

M.R.BATTAGLIA

ABSTRACT

Algorithms are described for the calculation and plotting of radar vertical coverage diagrams. Two contour VCD algorithms are presented, with a brief discussion on the problem of numerical stability, and the effects of ship motion and frequency agility.

POSTAL ADDRESS: The Director, RAN Research Laboratory
P.O. Box 706 Darlinghurst, N.S.W. 2010

CONTENTS

1. Introduction

Operational performance of Naval radars is routinely checked by measurement of the vertical coverage diagram (VCD). Comparisons of returns from a calibrated target with the VCD facilitates the detection of any degradation. This may be in the form of a lower average detection range or 'holes' in the vertical coverage. The former may result from electronic degradation or transmission line losses, while the latter may result from antenna damage or multipath effects - these being determined by sea state and choice of antenna height or operating frequency.

In reference 1, computer programs were described which calculated (i) the radar return from a target flying a specified height/range profile and (ii) the probability of paint for fluctuating and non-fluctuating targets. Refinements to the model, and the theoretical basis of the algorithms were outlined in reference 2.

Comparisons have been made between the output of these programs and the measured returns in the RAN sphere drop calibration trials. In the absence of ducting, any differences can generally be attributed to plumbing or other isotropic losses.

RANRL has been requested (ref 3) to produce programs suitable for desktop computers to solve the inverse problems - (i) the calculation of signal-to-noise required to yield a given probability of paint and (ii) the calculation and plotting of detection contours in a multipath environment. The ensuing sections describe the algorithms used in the programs.

2. The Radar Equation

The power returned in free space from a target of cross-section σ is given by the monostatic radar equation

$$P_r = \frac{P_t G^2 \lambda^2 \sigma}{(4\pi)^3 R^4} \qquad 1.$$

where P_t is the transmitted power, G is the power gain, λ is the radar wavelength and R is the target range. Multipath, diffraction and other environmental effects are accounted for by the pattern propagation factor (F) and the atmospheric loss factor (L)

$$P_r = \frac{P_t G^2 \lambda^2 \sigma F^4}{(4\pi)^3 R^4 L} \qquad 2.$$

The problem addressed in this paper is the calculation of F in equation 2, which may be recast to provide an expression for the maximum single-blip detection range:

$$R_{max} = \left[\frac{P_t G^2 \lambda^2 \sigma}{(4\pi)^3 P_n D_o L}\right]^{0.25} . F \qquad 3.$$

where P_t is the peak transmitted power and P_n is the system noise power. D_o is the single-pulse signal-to-noise ratio required to yield the desired probability of paint for a given number of pulses integrated, false alarm rate and target return statistics. In the absence of clutter, the limit to signal detectability is governed by the pulse energy, so that the effective noise power P_n, referred to the antenna, is determined by the transmitted pulse width (τ), the antenna noise temperature (T_a), the receiving line losses (L_r) and the receiver noise figure (NF)

$$P_n = k/\tau \left[T_a + T_r(L_r - 1) + L_r T_o(NF-1)\right] \qquad 4.$$

where T_r and T_o are the temperature of the receiving line and 290 K respectively, and k is Boltzmann's constant. If the receiver noise bandwidth B_n is used instead of $1/\tau$ in (4) the transmitted power should be multiplied by $B\tau$, the time-bandwidth constant, to give the effective S/N for probability of detection calculations. If clutter-to-noise is near unity, it is convenient to assume that the clutter-plus-noise variable ($P_c + P_n$) has the same statistical distribution as receiver noise, and this Rayleigh distributed total noise power is used for P_n in equation 3.

3. Required Signal-to-Noise

3.1 Approximate Formulae

There are numerous approximate formulae in the radar literature for evaluating paint probability from S/N (and vice versa). Reasonable estimates of detection range can be obtained using the simple formula suggested by Neuvy (ref 4):

$$D_o = 10 \log \left[\frac{\alpha}{N^{\gamma}} \cdot \frac{\log PFA}{(\log(1/P_d))^{\beta}} \right] \qquad 5.$$

where PFA is the probability of false alarm, P_d is the probability of paint, N is the number of pulses incoherently integrated. The detector law is described by the 'constant' γ which is often given the empirical value of 2/3 (ref 5) rather than the asymptotic limit of 1/2. Neuvy has given heuristic estimates of α and β for the Swerling and Marcum (non-fluctuating) targets as shown in Table 1.

Case	c	β
Swerling I	2/3[1 + 2/3 exp(-N/3)]	1
II	1	1/6 + exp(-N/3)
III	3/4[1 + 2/3 exp(-N/3)]	2/3
IV	1	1/6 + 2/3 exp(-N/3)
Non-fluctuating	1 + 2 exp(-N/3)	1/6

Table 1. Neuvy parameters for Marcum and Swerling targets.

	------ Swerling Case	------			
N	I	III	II	IV	Eqn (6)
1	10.5924	10.3747	10.5924	10.3747	10.5924
2	8.1681	7.9547	7.9547	7.9295	7.9547
3	6.8091	6.5984	6.5735	6.5938	6.7176
4	5.8732	5.6644	5.6443	5.6807	5.6060
5	5.1639	4.9565	4.9478	4.9907	4.8528
6	4.5949	4.3888	4.3926	4.4380	4.2808
7	4.1213	3.9163	3.9320	3.9781	3.8188
8	3.7165	3.5123	3.5392	3.5851	3.4310
9	3.3636	3.1601	3.1972	3.2425	3.0968
10	3.0511	2.8483	2.8947	2.9391	2.8030
20	1.0674	0.8689	0.9763	1.0105	0.9560
30	-0.0397	-0.2360	-0.0962	-0.0687	-0.0798
40	-0.8042	-0.9989	-0.8384	-0.8153	-0.8024
50	-1.3861	-1.5798	-1.4045	-1.3845	-1.3574
60	-1.8550	-2.0479	-1.8613	-1.8437	-1.8079
70	-2.2471	-2.4393	-2.2438	-2.2280	-2.1871
80	-2.5837	-2.7754	-2.5726	-2.5583	-2.5143
90	-2.8785	-3.0697	-2.8608	-2.8476	-2.8021
100	-3.1405	-3.3312	-3.1171	-3.1049	-3.0590
200	-4.8285	-5.0169	-4.7736	-4.7666	-4.7370
300	-5.7918	-5.9791	-5.7225	-5.7175	-5.7111
400	-6.4664	-6.6531	-6.3883	-6.3844	-6.3996
500	-6.9853	-7.1715	-6.9012	-6.8980	-6.9324
600	-7.4065	-7.5925	-7.3180	-7.3153	-7.3670
700	-7.7611	-7.9467	-7.6691	-7.6667	-7.7340
800	-8.0672	-8.2526	-7.9723	-7.9702	-8.0516

Table 2. Required signal-to-noise (dB) tabulated for N=1 to 800 pulses integrated (PFA=0.000001, P_d=0.33). Iterative solutions (columns 2-5) used fitted data in column 6 as 'first guess'.

These formulae are accurate to within a few dB for $0.1<P_d<0.9$ and moderate values of N. This range is not adequate since (i) the 95% contour is often specified as the required detectability contour and (ii) cumulative paint probability considerations might warrant the plotting of a $P_d<10\%$ contour. The formulae also do not give good agreement for $1<N<5$ which is typical for 3-D radar, nor are they applicable to very slowly fluctuating (Weinstock) targets. Expressions of comparable accuracy have been given by Albersheim (ref 6) and Blake (ref 7) for non-fluctuating targets.

3.2 Iterative Solutions

The formulae described above are not valid over a sufficiently large range of P_d, N, PFA and target scintillation rate to be used for routine VCD calculations, but are sometimes useful in providing a starting point for an iterative algorithm. However, in the unreliable regions (such as moderately large N and $P_d>90\%$) numerical instability poses a serious problem. A more robust starting point is required which covers the range of radar and target parameters likely to be encountered.

The method used here is based on the observation that D_o, for 33% probability of detection in gaussian noise, is virtually independent of the amplitude statistics of the target (see figure 1). Regression analysis of D_o data for $P_d=0.33$, $3<N<1000$, $PFA=10^{-6}$, Swerling case II, and non-coherent integration yields the following result

$$D_o = 7.138 + 1.018/\log(N) - 5.533.\log(N) \qquad 6.$$

with D_o in dB. Values for N=1 and 2 are evaluated separately in the program.

The secant iterative method with equation 6 as first guess, together with the algorithms of reference 2, were used to produce the data in table 2. Iteration was stopped at $P_d = 0.33\pm0.00001$. The accuracy of equation 6 is of the order of the dependence on target scintillation (±0.1 dB) at 33% probability of detection. Results for 50% and 95% ($\pm$ 0.001%) are shown in graphical form in figures 2 and 3.

4. The Radar VCD

In free space, the detectability contour, or vertical coverage diagram, is determined by equation 3 with F replaced by the antenna pattern function $f(\theta)$

$$R_{max} = f(\theta).R_o \qquad 7.$$

where R_o is the detection range along boresight, and θ is the elevation angle. This smoothed contour is also useful for estimating mean detection ranges at higher elevation angles and moderate sea states, in which case the multipath structure is washed out (see also later section on ship motion). At lower elevation angles, or sea states, multipath lobing must be considered and the detection contour becomes

$$R_{max} = F.R_0 \qquad 8.$$

Under non-ducting conditions, the pattern propagation factor, F in the interference region is

$$F = f(\theta_1).\sqrt{1 + x^2 + 2x \cos \phi} \qquad 9.$$

and may take values between 0 and 2. The phase difference ϕ is the sum of contributions from the geometric path difference between the direct and indirect rays (fig 4), and the phase difference on reflection from the sea surface of the indirect ray. The reflectivity parameter x is

$$x = \frac{r\ \rho\ D\ f(\theta_2)}{f(\theta_1)} \qquad 10.$$

in which D is the divergence factor, r is the roughness factor, ρ is the dielectric reflectivity (the reflectivity which would apply if the sea were perfectly smooth) and θ_1 and θ_2 are as shown in figure 4.

For elevation angles near the horizon, and for targets over the horizon, F is calculated using diffraction theory (or by interpolation as described in ref 1) with

$$F = f(\theta_1).\sqrt{U(X).V(Z_1).V(Z_2)} \qquad 11.$$

where X, Z_1, Z_2 are range, target height and antenna height respectively in natural units and the functions V and U are gain functions described in reference 2.

4.1 VCD Envelope

The main features of the VCD for Naval radars can be calculated using ray theory. The envelope of R_{max} is obtained with equations 8 and 9 with

$$\phi_{max} = 2\pi m \qquad (m=1,2,3......) \qquad 12.$$

so that,

$$R_{max}(\text{envelope}) = f(\theta_1).(1+x).R_0 \qquad 13.$$

Within the range of elevation and grazing angles of interest, the shape of the VCD is thus dominated by $f(\Theta)$ and r.

4.2 The Roughness Factor

The reflectivity of the indirect ray can be written as

$$\Gamma = r.\rho.e^{-j\emptyset} \qquad 14.$$

where r is the roughness factor, and ρ and $\emptyset$ are the magnitude and phase respectively of the specular reflection coefficient. Formulae for ρ and $\emptyset$ as functions of grazing angle, frequency, water temperature and salinity are given in reference 2 and are in good agreement with experimental data. The dependence of the roughness factor on grazing angle and frequency is less straightforward, and there is a paucity of experimental data.

Ament (ref 8) has shown that if the wave height distribution is gaussian, (variance σ^2), then the surface roughness will also be gaussian

$$r = e^{-2s^2} \qquad 15.$$

where

$$s = 2\pi\sigma.\sin\gamma/\lambda \qquad 15a.$$

This equation gives good agreement at low grazing angles (γ), but this is to be expected since r-->1 as γ-->0. That is, most models will predict Γ_{max}~$2R_0$ for the lowest multipath maximum over a wide range of frequencies and sea states, despite the lack of agreement for the high altitude coverage.

At higher values of s the reflection is not purely specular. The additional diffuse component adds to the fluctuation in the pattern propagation factor, but not to its average value. The random component of F is not considered in the program, but rather an effective constant value is assumed. Reasonable agreement for large s is obtained using the empirical expression given in reference 1:

$$r = e^{-2s^2} \quad \text{for } r>0.44 \qquad 16.$$
$$= e^{-1.2732s} \quad r<=0.44$$

The program also makes use of the Burling relationship between significant wave height ($H_{1/3}$)and σ

$$H_{1/3} = 4\ \sigma \qquad 17.$$

4.3 Antenna Pattern Functions

At high elevation angles and moderate sea states x→0 and the envelope of F_{max} is dominated by the APF, as per eqn 7. Elsewhere, the antenna pattern function of both the direct and indirect rays are required for the calculation of F. In general, the APF needs to be represented adequately out to the first sidelobe. The program calculates either (i) a cosecant-squared pattern or (ii) a modified sin u/u fan beam of the form

$$f(\theta) = \frac{\sin \pi\sqrt{u^2 - B^2}}{\pi\sqrt{u^2 - B^2}} \qquad 18.$$

where u=d.sinθ/λ and B is a constant for the antenna, which describes the sidelobe level and aperture efficiency. Methods for calculating B from the sidelobe level are described in reference 2

5. Graphical Representation of VCD

In the absence of pitch and roll the VCD is independent of radar azimuth (neglecting blind arcs and superstructure multipath) so that the VCD can be displayed as a 2-D graphical representation. Variations with range and height of paint probability or signal-to-noise can be described by an arbitrary number of grey scales.

In figures 5-8, the VCD of a UHF air search radar and a G-band surface search radar are illustrated for two sea states. Gross parameters used for the UHF radar are λ = 0.7 metre, antenna height h_1 = 30 metre, N=75 pulses incoherently integrated, sea states 0 and 6, and a free space range of R_0 = 80 n.miles against a 1 metre-squared target. Parameters used for the G-band radar are λ = 0.05 metre, h_1 = 25 metre, N = 5, sea states 0 and 3 and R_0 = 17 n.miles. Standard atmospheric conditions and scan-to-scan (Swerling case I) target scintillation are assumed. The grey scales correspond to paint probability regions P>95%, 50%<P<95%, 5%<P<50% and P<5%, and were computed as described in the previous section.

The VCD's were produced by taking 120 cuts in height for 200 range increments. Sea clutter was included in the noise calculations, using the expressions described in reference 2 For reasons of clarity the plots are not truncated at minimum range and maximum unambiguous range as determined by the radiated pulse width and PRF respectively. In order to resolve the structure in the G-band plots, calculations were carried out only to 4000 feet and limited to sea state 3, while the UHF calculations were carried out to a height sufficient to contain the 5% probability contour.

The calculations for figures 5-8 took a few minutes of processing time on a CDC Cyber 76 mainframe computer. Such a program is however unsuitable for small desktops, such as the Tektronix Graphics System specified in reference 3, since similar calculations would take 2-3 days of computer time for each plot. The next section describes methods for producing line contour VCD s which can be quickly computed on a small desktop machine, using a modification of the program described in ref 1

6. Contour Plotting

6.1 Asymptotic Behaviour The Flat Earth Limit

Fast algorithms for computing contour VCD s are not easily implemented due to the lack of symmetry in the multipath lobing structure. One method often employed is to perform an approximate calculation of the VCD using the flat earth multipath results and to modify the computed results graphically or by scaling to account for curvature Even this approach however will not be generally applicable due to the additional geometric approximations that must be made.

In the flat earth limit D=1 and, for horizontally polarized UHF radars at low to moderate elevation angles, r=1 and the phase difference on reflection is π radians The path difference between direct and indirect rays for a target at ground range G is

$$\delta = \sqrt{(h_1+h_2)^2 + G^2} - \sqrt{(h_2-h_1)^2 + G^2}$$

If the free space range of the radar is large compared with the sum of target and antenna heights the path difference for constructive interference is given approximately as

$$\delta = \frac{2h_1h_2}{R\cos\theta} \qquad 19.$$

Within the antenna main lobe (f(0)~1) the pattern propagation factor then simplifies as

$$F = 2\left[\sin(2\pi h_1 h_2/\lambda G)\right]$$

$$= 2\left[\sin\frac{2\pi h_1}{\lambda}\left(\tan\theta + \frac{h_1}{G}\right)\right] \qquad 20.$$

Usually $G \gg h_1/\tan\theta$ for naval search radars at ranges of interest, so that the VCD's produced from the flat earth model are highly symmetric - that is, only one calculation of multipath geometry need be performed for one range at each elevation angle increment, with R^{-4} scaling to determine the range for a specified probability of detection and false alarm rate (using the algorithms of section 3). A first order correction for the effect of the earth's curvature can be included after the last approximation. This is equivalent to assuming that the sea surface is flat up to the point of reflection so that the final result requires only the transformation $h_2 \to h_2 + G^2/2a_e$.

The algorithms used in the program described here do not rely on the flat earth model, however the gross structure of the VCD can be determined using the procedure described above. Such a description is therefore a useful basis for a more general algorithm.

6.2 Spherical Earth Model
- Dependence of F on Range

The flat earth model predicts that the lobe maxima for long range naval radars occur (with F=2) at elevation angles

$$\theta_{max} = \sin^{-1}(2m-1)\lambda/4h_1 \qquad m=1,2,3,.... \qquad 21.$$

It is clear from figures 5-8 that, in the more general model, F=2 at the lobe maxima only at low elevation angles. This implies, not only that twice the free space range will be achieved only at lower altitude, but also that the lobe spacing is not uniform. Equation 21 is, however, useful for determining the elevation angle spacing required to fully resolve the multipath structure. In the program, ten points are calculated per nominal lobe spacing. This facilitates both resolution of the lobes and the ability to read the radar range from the plots to a within a few percent of R_c.

The behaviour at constant elevation angle for a spherical earth is most easily demonstrated graphically. Figures 9 and 10 are typical plots of the signal return for the UHF radar described in the previous section. The plots are for a 1 metre-squared target at two intermediate elevation angles, separated by half a nominal lobe spacing, at sea states 0 and 6. If the free space range of the radar is large compared with the clutter horizon, algorithms for contour VCD s are likely to be most stable at higher sea states due to the reduced multipath lobing. This is seen in the plot for sea state 6 (figure 10) where results for both elevation angles yield results which are close to the free space result. Since the power return decays as the fourth power of range, either a scaling or iterative algorithm should calculate the required signal-to-noise in one or two iterations even if the first inaccurate.

The behaviour at low sea states is less well b robust algorithms are generally required. In figure 9 t at the free space range (80 n.miles) is qualitatively di two elevation angles selected. One curve corresponds t of a lobe maximum (at 80 n.miles) and R^{-4} behaviour is s 2.0 times the free space range. This type of behaviour is and implies that as long as the first guess for long around the free space range, the detection range ($S/N=D_o$ maxima will generally be easily computed. At very sho hopping occurs for constant elevation angle calculations s algorithms may be numerically unstable.

As a corollary, iterative algorithms may be uns range search radars such as the G-band radar of the previc the worst case there may be either no solution or severa $S/N=D_o$ at a given elevation angle. The former case may ap sea states if the detection range is of the order of the c while the latter will be worst at low sea states where lobing is most pronounced.

6.3 Description of Main Program

Either of two algorithms may be selected in the ma cases where numerical stability is not a problem the pref calculation is an iterative search method. This algorit reliable results at moderate sea states for naval radars is large compared with the clutter horizon. This method there is a solution along a selected elevation angle and is reasonable (power monotonically decreasing with ra detection range can be calculated with arbitrary preci sensitivity of 0.25 dB should be acceptable for most app 10 points are plotted per nominal lobe spacing.

In order to increase the probability of the searc numerically stable region, the first two corrections to th are scaled assuming R^{-4} and R^{-8} decay law respectively reduce ringing), with subsequent iterations independent of If a solution has not been obtained by a specified numbe the 'solution' plotted will correspond to the minimum val This method will therefore produce reliable ranges in structure but not necessarily in the nulls. This loss of of little consequence (see figures 5-8) especially considering that the power in the nulls is highly variable due to ship motion (discussed in next section) , wave height fluctuations, atmospheric inhomogeneity, and other factors.

The second algorithm is a one-step scaling algorithm, so that the computed detectability range, at a specified elevation angle, will in general be reliable only if the first guess is close to the actual detectability range. The scaling algorithm in the program is optimized to produce a reliable envelope for VCD contour since the first guess at any elevation angle is the range to the lobe maximum, given by equation 13. Since the reflectivity parameter x is a function of R, it is not known until the final solution is obtained. An estimate $\hat{x}$ is used, and this provides an estimate $\hat{R}_{max}$:

$$\hat{R}_{max} = R_0 \ f(\Theta).(1+\hat{x}_i) \qquad 22.$$

The estimate $\hat{x}_i$ is the value corresponding to the last solution (x_{i-1}). With this procedure, R_{max} will be calculable to within a few percent at sea state 0 if at least 10 points are calculated per multipath lobe. At higher elevation angles and/or sea states the multipath lobing structure is washed out (x_i-->0) so that this algorithm will be both robust and accurate if R_0 is greater than the clutter horizon.

Plots using these algorithms are given in plots 11-17. The contour selected is 0 dB in all cases, which corresponds to 4% and 52% probability of paint for the G-band (N=5) and UHF (N=75) radars respectively against a Swerling case I, 1 metre-squared target . Figures 11 and 12 used the iterative algorithm (0.25 dB sensitivity) at sea states 0 and 6. The contour VCD's are in good agreement with the grey scale envelopes of figures 5 and 6. An additional plot for sea state 3 (fig 13) is included to illustrate the gradual, and very significant, decrease in maximum height with sea state. The same parameters were used to produce the plots in figures 14 and 15 with the scaling algorithm. Although this algorithm is optimized at the lobe maxima, it also gives good agreement in the mid-lobe region. The lower half of each lobe is generally well reproduced to much shorter ranges - this is fortuitous since this is the lobe region of interest for inbound air targets.

Figure 16 and 17 show the results of the scaling algorithm for the G-band contours, with the calculations stopped at an elevation angle corresponding to the maximum height in the full graphical representations (fig 7-8). Again, the 0 dB contour (4%) is consistent with the 5% grey scale envelope of figures 7-8. With this radar, the pattern propagation factor has a stronger range-dependence so that the iterative algorithm is numerically less stable. The manifestation of this is a VCD with a much higher incidence of 'bad' data points (about 5% of all points calculated). At sea state 0, the lobes for this radar are pronounced but closely spaced so that only the envelope of the VCD contour is easily measured (sufficient reason for using the quicker scaling method). At higher sea states the effect of ship motion further complicates the VCD.

7. Effect of Ship Motion

The motion of the ship is most conveniently described in terms of the reference axes systems defined in figure 18. A natural choice for the 'space-fixed' axis system utilizes the mean sea surface as the x-y plane. The ship's axis system is also naturally defined by the effective plane of symmetry through the keel, which is defined as the x'-z' plane, with the y'-axis passing through the antenna.

Relative motion of the two axes systems about the vertical (yaw) is equivalent to a fluctuation in the antenna rotation rate and, thus, the number of pulses integrated. Similarly, the number of hits per scan is increased or decreased during a rapid turn. Although this motion may be of the same order as the normal antenna motion, the probability of detection is only a weak function of the number of pulses incoherently integrated, and can therefore be ignored in most cases. Motion of the ship in the x-y plane is also ignored since the VCD is plotted in terms of relative range which will not change significantly during the time on target for normal antenna rotation rates and target range rates.

Pitch and roll can be defined as the angles Θ and $\emptyset$ respectively in figure 18. The effects of ship 'rotation' are symmetric in pitch and roll unless a specific target bearing is considered. For a target on the bow, pitch has the same effect as varying the antenna tilt in the x,y,z axis system while preserving the polarization of the radiation. (The effect of the vertical motion of the antenna during pitch/roll is discussed later in the section on heave). Pitch or roll can be significant compared with vertical beamwidth, even for wide beamwidth search radars. This not only has the effect of increasing the maximum angle of the main antenna lobe VCD, but also gives rise to calculable fluctuations in the pattern propagation factor at moderate elevation angles due to variations in the APF of the direct and indirect rays. This is shown in figure 19, where the antenna tilt was allowed to vary randomly between zero and 10% of the vertical beamwidth.

The effect of roll for a target along zero relative bearing also has a small azimuth fluctuation effect for targets at moderate elevation angles. (This effect is not normally significant, or else it would provide an elegant method of determining target elevation using a 2-D radar.) A second effect for this relative geometry is that polarization of the radiation in the space-fixed system is partially converted to the opposite sense. The detecting antenna is only concerned with the polarization in the ship's axis system, so that this is only manifested through multipath effects. Six degrees of roll converts only 1% of the radiation to the opposite polarization. At grazing incidence for the indirect ray, the phase difference and reflectivity are near π and 1 respectively for both polarizations, so that the lowest lobe is virtually independent of polarization. At moderate elevation, the magnitude and phase for vertical polarization may be sufficiently different to put maxima at the elevation angle of a minimum for the opposite polarization. Since the detection range is of the order of $(S/N)^{0.25}$, the nulls for a 1% polarization change may be filled to about a third of the range for the adjacent lobe maxima.

In the case of heave, the effect is simply related to the ratio of heave to mean antenna height above sea level. A simulation of the effect of heave is shown in figure 20 (one run only), where the antenna height was uniformly distributed over the nominal heave dimension. The effect on the lower lobes is only slight, but heave has the effect of filling in the upper lobes and thus reducing the mean detection range along a lobe maximum. If the mean of many simulation runs is calculated for each elevation angle, the nulls at the n-th lobe will be completely filled if n is of order (antenna height/2.heave) or greater, decreasing in effect with decreasing elevation angle.

Ship heave will also affect the probability of detection by its effect on the target fluctuation statistics. In the case of slowly fluctuating (Weinstock) targets, heave will modify the scintillation to scan-to-scan (Swerling case I) at higher elevation angles but will have a reduced effect on the amplitude statistics at lower angles. Targets with Swerling case I-IV statistics will not be affected to the same extent since ship motion is negligible on a pulse-to-pulse timescale for typical PRF's.

8. Frequency Agility and Diversity

The radars discussed above are assumed to have a transmitted frequency bandwidth of order of the inverse of the pulsewidth - typically 1 MHz. With pulse compression radar it is the inverse of the compressed pulsewidth. In addition, the centre frequency may be tuned over a range of several percent - typically tens of MHz. The single-pulse bandwidth is small compared with the centre frequency, and so has no significant affect on the VCD, while the tunability of the radar set simply changes the number of lobes that fit into the antenna main lobe at fairly long time intervals. (The frequency term in the radar equation can be assumed to be a constant, since the detection range varies as the square root of the wavelength.)

Frequency agility has an analogous effect on the radar VCD. The detectability, averaged over all transmitted frequencies, may be the same as a simple tunable radar, however on a scan-to-scan timescale the radar VCD's are quite different. The elevation angle to the n-th lobe is approximately proportional to the ratio of the transmitted wavelength to the antenna height. If the agility was random, and on a scan-to-scan basis, the effect on the VCD would be similar to the heave simulation in figure 20. That is, the lower lobes would be unaffected but the power in the upper lobes would be fluctuating about the free space level. Pulse-to-pulse random agility yields the same mean detection range but the fluctuations are averaged out in the integration process. A second effect of random pulse-to-pulse frequency agility is on the number of independently fading signal groups per scan, or alternately the number of degrees of freedom of the equivalent Chi-square target. If F frequencies are transmitted per scan with sufficient separation to have independent echoes, then a target which is represented as having 2K degrees of freedom for the fixed frequency radar has up to 2KF degrees of freedom for the pulse-to-pulse frequency agile radar (K=F,N,2F and 2N for Swerling cases I,II III and IV respectively).

Acknowledgement.

Helpful suggestions from LtCdr P Williams are acknowledged.

REFERENCES

1. Battaglia, M.R. (1983). RAN Research Laboratory. A Computer Program for the Prediction of Search Radar Performance. (U) RANRL Tech Note (Ext) 1/83. UNCLASSIFIED.

2. Battaglia, M.R. and P.Williams (1983). RAN Research Laboratory. A Model of Radar Propagation and Detection.(U) RANRL Tech Note (Ext) 2/83. UNCLASSIFIED.

3. RANTAU Minute 59-17-2 (DS) , 7th Sept 1983 (R).

4. Neuvy,J. (1970) 'An Aspect of Determining the Range of Radar Detection', I.E.E.E. Trans on Aerospace and Electronic Systems, AES-6 (4), p 514.

5. Brookner,E (Ed) (1977).<u>Radar Technology</u>, Artech, Dedham, p 387.

6. Tufts, D.W. and A.J.Cann (1983). 'On Albersheim's Detection Equation', I.E.E.E. Trans on Aerospace and Electronic Systems, AES-19 (4), p 643.

7. Blake, L.V. (1980). <u>Radar Range Performance Analysis</u>, D.C.Heath and Co., Lexington.

8. Ament, W.S. (1953). 'Toward a Theory of Reflection by a Rough Surface', Proc. I.R.E., 41(1), p 142.

ANNEX A

Calculation of Detection Threshold For Fixed Threshold Detectors

```
1201   REM ****************************************************************
1205   REM UTILITY ROUTINE TO CALC SUM N0=0 TO N-1 OF Y0^M.e^-Y0/M!
1206   DEF FN LGT(X)=LOG(X)/LOG(10)
1210   IF N>1 GOTO 1215
1211   Y2=EXP(-Y0)
1212   RATIO=1.0
1213   GOTO 1280
1215   N0=0:ANSWER=0
1216   LIMIT=1.0E35
1217   IF Y0>1 THEN Y1=Y0*10^(37- FN LGT(Y0)):ELSE Y1=1/Y0*10^(37+ FN LGT(Y0))
1220   FACTOR=-LOG(Y1)
1225   REM START OF MAIN LOOP
1230   FACTOR=FACTOR+LOG(Y1)*2
1235   Y1=1/Y1
1240   IF N0=0 THEN Y2=Y1:ELSE Y2=0
1245   REM START OF INNER LOOP
1250   N0=N0+1
1255   Y1=Y0/N0*Y1
1260   Y2=Y2+Y1
1265   IF(N0<(N-1)) AND(Y2<LIMIT) GOTO 1245
1270   ANSWER=ANSWER+EXP(LOG(Y2)+FACTOR-Y0)
1275   IF N0<(N-1) GOTO 1225
1276   IF Y1>0 THEN RATIO=EXP(LOG(ANSWER)+Y0-FACTOR-LOG(Y1))
1278   Y2=ANSWER
1280   RETURN
1290   REM ****************************************************************
1320   REM START OF MAIN ROUTINE TO CALCULATE THRESHOLD (Y0) FROM N AND PFA
1330   Y0=-1*LOG(PFA)
1335   RATIO=1.0
1340   IF N<=1 THEN 1410
1350   REM First estimate for Y0
1360   Y0=(SQR(-LOG(PFA))+SQR(N)-1)*SQR(-LOG(PFA))+N-SQR(N)
1370   GOSUB 1201
1380   D0=LOG(Y2/PFA)*RATIO
1390   Y0=Y0+D0
1400   IF ABS(D0/Y0)=>3.0E-7 THEN 1370
1410   REM Y0 IS THRESHOLD FOR FIXED THRESHOLD DETECTOR
1420   RETURN
1425   REM ****************************************************************
```

ANNEX B

Calculation of Pd for Marcum, Swerling and Weinstock Targets

```
1425   REM ****************************************************************
1430   REM CALCULATE Pd FROM S/N (X dB),CHI-SQUARE PARAMETER (K),N AND YO
1440   ELIMIT=1/(10*N):Y2=PFA
1443   Y1=PFA/RATIO
1444   NO=N
1450   X=10^(X/10)
1460   S1=Y2
1470   X1=(K/(K+N*X))^K
1480   X2=X1
1490   X3=X*N/(K+N*X)
1500   D1=K-1
1510   M=1
1520   R1=0
1525   IF X2=0 THEN GOSUB 1661
1526   REM RESUME AFTER UNDERFLOW LIMIT REACHED
1530   L1=R1
1540   Y1=Y1/NO*YO
1550   Y2=Y2+Y1
1560   S1=S1+Y1*(1-X2)
1570   E1=(1-X2)*(1-Y2)
1580   R1=S1+E1
1590   X1=(D1+M)/M*X1*X3
1600   X2=X2+X1
1605   IF(X2>1) THEN X2=1
1610   M=M+1
1620   NO=NO+1
1630   IF ABS(1-L1/R1)=>3.0E-7 THEN 1530
1640   IF E1=>ELIMIT THEN 1530
1650   REM R1 IS THE PROBABILITY OF DETECTION
1655   RETURN
1656   REM ****************************************************************
1660   REM SUBROUTINE TO SCALE FOR UNDERFLOW
1661   X4=0:X5=K*(LOG(K)-LOG(K+N*X))
1662   X6=LOG(X3)
1663   REM JUMP HERE TILL LIMIT
1664   Y1=Y1/NO*YO
1665   Y2=Y2+Y1
1666   S1=S1+Y1
1667   X4=X4+X6+LOG(D1+M)-LOG(M)
1668   X1=EXP(X5+X4)
1669   X2=X2+X1
1670   M=M+1
1671   NO=NO+1
1672   IF X2=0 THEN GOTO 1663
1673   RETURN
1675   REM ****************************************************************
```

ANNEX C

Calculation of Required Signal-to-Noise (Do)

```
8000    REM *******************************************************************
8001    REM routine to solve roots of f(x)=R1 by secant method
8002    REM SNdBn IS CURRENT ESTIMATE IN dB OF S/N REQUIRED FOR Pd = PROB
8003    DEF FN LGT(X)=LOG(X)/LOG(10)
8004    LN= FN LGT(N)
8005    REM
8006    PROB=0.95
8007    PROBLIMIT=0.00001
8008    REM ITERATION WILL BE STOPPED WHEN SNdB3 = PROB +/- PROBLIMIT
8010    REM FIRST ESTIMATE OF REQUIRED S/N IS FIT OF SOLUTIONS FOR PD=0.33
8011    IF N<3 THEN SNdB3=10.5924-8.74904*LN
8012    IF N>=3 THEN SNdB3=7.138+1.018/LN-5.353*LN
8013    SNdB3=SNdB3+4.343* FN LGT(PFA/1.0E-6)/ FN LGT(PFA)
8014    REM SECANT METHOD SEEDED WITH 2 POINTS STRADDLING Pd=0.33
8015    SNdB1=SNdB3-1.0:X=SNdB1:GOSUB 1430:PROB1=R1
8020    SNdB2=SNdB3+1.0:X=SNdB2:GOSUB 1430:PROB2=R1
8025    REM
8028         IF(PROB2=0) AND(PROB1=0) THEN SNdB3=SNdB3+0.25:GOTO 8015
8029         IF(PROB2=1) AND(PROB1=1) THEN SNdB3=SNdB3-0.25:GOTO 8015
8030    SLOPE=(SNdB2-SNdB1)/(PROB2-PROB1)
8035    TESTSLOPE=(PROB-PROB2)*SLOPE
8036         IF TESTSLOPE>3 THEN SNdB3=SNdB2+ FN LGT(TESTSLOPE):GOTO 8050
8037         IF TESTSLOPE<-3 THEN SNdB3=SNdB2- FN LGT(-TESTSLOPE):GOTO 8050
8040    SNdB3=SNdB2+TESTSLOPE
8050    X=SNdB3:GOSUB 1430:PROB3=R1
8055    REM   SNdB3 IS CURRENT ESTIMATE OF Do FOR Pd=100*PROB3 %
8060    IF ABS(PROB3-PROB)<PROBLIMIT THEN GOTO 8100
8070    SNdB1=SNdB2:PROB1=PROB2
8080    SNdB2=SNdB3:PROB2=PROB3
8090    GOTO 8030
8100    PRINT "ITERATION STOPPED  AT ";SNdB3;" dB = ";100*PROB3;" %"
8110    RETURN
9000    REM ***************************************************************
```

ANNEX D

Calculation of Paint Probability for Non-fluctuating Targets

```
1425   REM ****************************************************************
1430   REM **** PROBABLILTY OF DETECTION FOR NON-FLUCTUATING TARGETS***
1431   REM CALCUATION OF Pd AT : Signal-to-Noise = X dB
1432   REM                        Probability of False Alarm = PFA
1433   REM                        N Pulses Non-coherently Integrated
1444   REM                        Fixed Threshold = Y0
1445   REM
1440   Y2=PFA
1443   Y1=PFA/RATIO
1444   N0=N
1450   X=10^(X/10)
1460   S1=Y2
1465   X3=N*X
1470   X1=EXP(-X3)
1480   X2=X1
1492   X6=LOG(X3)
1510   M=1
1520   R1=0
1525   REM TEST FOR UNDERFLOW CONDITION
1526   IF X2=0 THEN GOSUB 1661
1530   L1=R1
1540   Y1=Y1/N0*Y0
1550   Y2=Y2+Y1
1560   S1=S1+Y1*(1-X2)
1570   E1=(1-X2)*(1-Y2)
1580   R1=S1+E1
1590   X1=X3/M*X1
1600   X2=X2+X1
1610   M=M+1
1620   N0=N0+1
1630   IF ABS(1-L1/R1)=>3.0E-7 THEN 1530
1640   IF E1=>0.001 THEN 1530
1650   REM R1 IS THE PROBABILITY OF DETECTION
1655   RETURN
1656   REM ******************************************************************
1660   REM USE SCALING ROUTINE WHILE UNDERFLOW CONDITION EXISTS
1661   X4=0
1662   X6=LOG(X3)
1663   REM JUMP HER TILL LIMIT
1664   Y1=Y1/N0*Y0
1665   Y2=Y2+Y1
1666   S1=S1+Y1
1667   X4=X4+X6-LOG(M)
1668   X1=EXP(X4-X3)
1669   X2=X2+X1
1670   M=M+1
1671   N0=N0+1
1672   IF X2=0 THEN GOTO 1663
1673   RETURN
1674   REM *********************************************************;**********
```

ANNEX E

Main Program for Contour VCD calculations.

```
1    REM DEFINE FUNCTIONS REQUIRED FOR GEOMETRY ROUTINES
6    DEF FN LGT(X)=0.43429448*LOG(X)
7    DEF FN ASN(X)=ATN(X/SQR(1-X^2))
8    DEF FN SL(X)=SQR((HH2-HH1)^2+4*(A1+HH1)*(A1+HH2)*(SIN(X/(2*A1)))^2)
9    DEF FN GR(X)=2*A1* FN ASN(SQR(((X^2-(HH2-HH1)^2)/(4*(A1+HH1)*(A1+HH2)))
12   DEF FN EL(X)= FN ASN((2*A1*(HH2-HH1)+HH2^2-HH1^2-X^2)/(2*(A1+HH1)*X))
13   DEF FN IND(X)= FN ASN((2*A1*HH1+HH1^2+X^2)/(2*(A1+HH1)*X))
2190 REM  VCD ALGORITHM IS ITERATIVE OR R^4 SCALING ( I OR S )
2196 REM 30 MULTIPATH LOBES CALCULATED USING DEFAULT PARAMETERS (POINTS%=300
2199 REM ****************************************************************
2200 REM START OF MAIN PROGRAM
2201 R7=SQR(2*A1/M1)*(SQR(H1))
2202 MINELEV=-1.0* FN ASN(H1M/R7+R7/2/A1):MAXELEV=TILT+1.1*B1
2203 PRINT"MIN ELEVATION = ";57.3*MINELEV;"  DEGREES"
2204 DBLIMIT=0.25:REM 0.25 dB RESOLUTION FOR ITERATIVE ALGORITHM
2205 PRINT"CALCS CARRIED OUT TO ";57.3*MAXELEV;"  DEGREES"
2206 INCELEV=0.1* FN ASN(W/(2*H1))
2207 ELTHETA(1)=0.70*MINELEV
2208 PRINT"USING LOOKUP TABLE PROVIDED,WHAT IS THE SIGNAL-TO-NOISE RATIO"
2209 PRINT"REQUIRED FOR THIS RADAR'S VCD CONTOUR":INPUT THRESH
2210 LINP1=10^(P1/10)
2211 QTHRESH=10^(-THRESH/40):R0=R0*QTHRESH
2212 FOR I=1 TO POINTS%
2213   FIRSTSLANT=ABS(R0*F1*(1+R1*F2/F1))
2214   IF I=1 THEN GOTO 2220
2215   ELTHETA(I)=ELTHETA(I-1)+INCELEV
2216   IF ELTHETA(I)>MAXELEV THEN I=POINTS% :GOTO 2400
2220   THETA=ELTHETA(I):GOSUB 920
2225   REM First estimate of range
2227   SLANT=FIRSTSLANT
2240   PRINT" FIRST SLANT = ";SLANT
2242   LOWLIMIT=10
2245   ITERATION=0
2250   REM ark** Compute  first estimate of altitude
2251   IF ALG$="I" GOTO 2255
2252   IF ITERATION=2 GOTO 2375
2255   HH1=H1M
2257   H9(I)=SLANT^2+2*SLANT*(A1+HH1)*SIN(ELTHETA(I))+(A1+HH1)^2
2258   H9(I)=M1*(SQR(H9(I))-A1)
2260   PRINT"HEIGHT = ";H9(I);" FEET"
2261   HH1=H1M:HH2=H9(I)/M1:G(I)= FN GR(SLANT)
2262   H2=H9(I)
2263   G8=G(I)
2265   ITERATION=ITERATION+1
2270   R7=SQR(2*A1/M1)*(SQR(H1)+SQR(H9(I)))
2280   REM  Compute target multipath geometry
2290   GOSUB 2680
2300   REM       Compute clutter return for ith point - C7(I)
2310   GOSUB 3400
2320   REM    Calculation/interpolation of pattern propagation factor - F(I)
2330   GOSUB 2470
2340   REM    radar  equation
2350   F(I)=K6+F(I)+RCS-40* FN LGT(SLANT)-2*L3*SLANT
```

Main program (cont'd)

```
2352      NOISE=10* FN LGT(LINP1+(10^(C7(I)/10)))
2353      INCSLANT=SLANT-OLDSLANT
2354      OLDEXCESS=EXCESS:OLDSLANT=SLANT
2355      EXCESS=F(I)-NOISE:IF ABS(EXCESS-THRESH)<DBLIMIT THEN GOTO 2375
2356      INCEXCESS=EXCESS-OLDEXCESS
2357      IF(ABS(EXCESS-THRESH)>ABS(LOWLIMIT)) THEN GOTO 2359
2358      LOWLIMIT=EXCESS-THRESH:LOWG=G(I):LOWR=OLDSLANT:LOWH=H9(I):LOWP=F(I)
2359      IF ITERATION<10 THEN GOTO 2365
2360      EXCESS=LOWLIMIT+THRESH:G(I)=LOWG:OLDSLANT=LOWR:H9(I)=LOWH:F(I)=LOWP
2361      GOTO 2375:REM END ITERATION AND USE SMALLEST EXCESS IN VCD
2362      IF ITERATION<2 THEN SLANT=SLANT*QTHRESH*(10^(EXCESS/40))
2363      IF ITERATION<2 THEN GOTO 2369
2365      IF ITERATION<4 THEN SLANT=SLANT*(QTHRESH*(10^(EXCESS/40)))^0.5
2366      IF ITERATION<4 THEN GOTO 2369
2367      SLANT=SLANT+(THRESH-EXCESS)*INCSLANT/INCEXCESS
2368      IF SLANT<0 THEN SLANT=2*R0*RND(1)+0.0811*W5
2369      PRINT"SLANT= ";OLDSLANT;" ELEV= ";57.3*ELTHETA(I);" EXCESS= ";EXCESS;
2370      PRINT:GOTO 2250
2375      RSLANT(I)=OLDSLANT
2380      REM  Printout
2390      GOSUB 2840
2395      IMAX=I
2400      NEXT I
2450      REM ******************************************************************
```

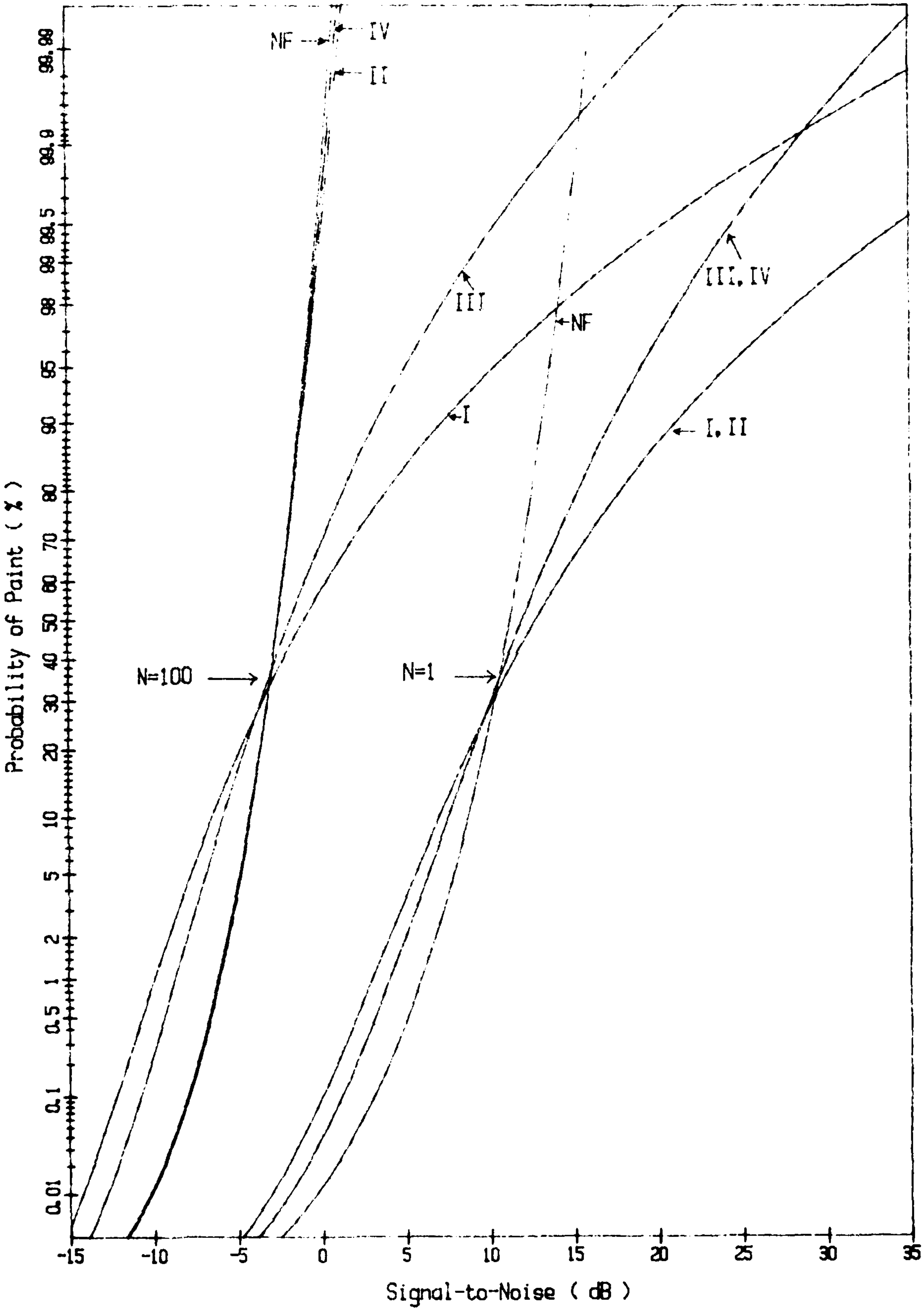

Figure 1. Probability of paint for Swerling case I - IV and non-fluctuating targets. PFA=0.000001, N=1 and N=100.

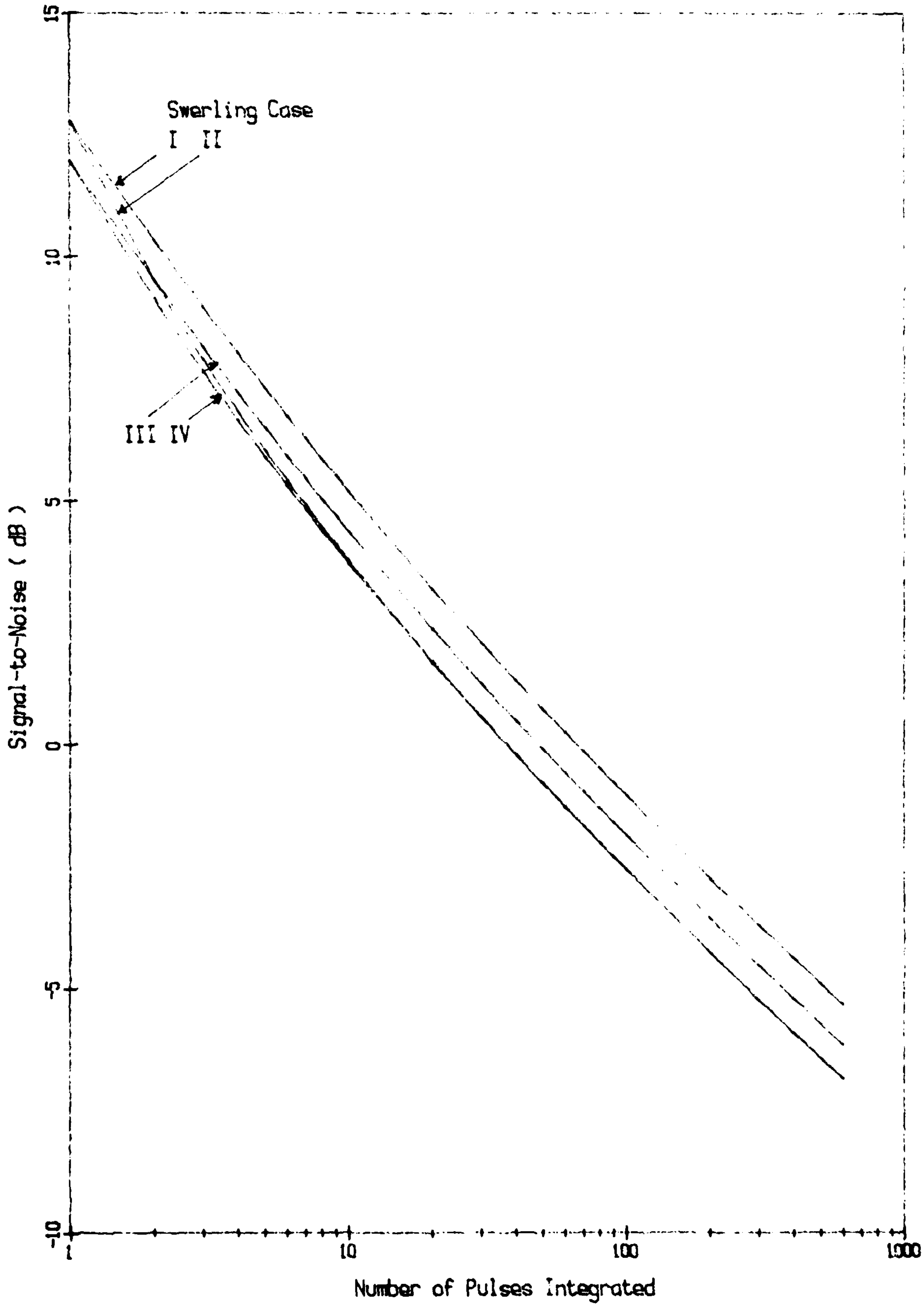

Figure 2. Signal-to-noise required for 50% paint probability.
PFA = 0.000001. Swerling case I-IV targets.

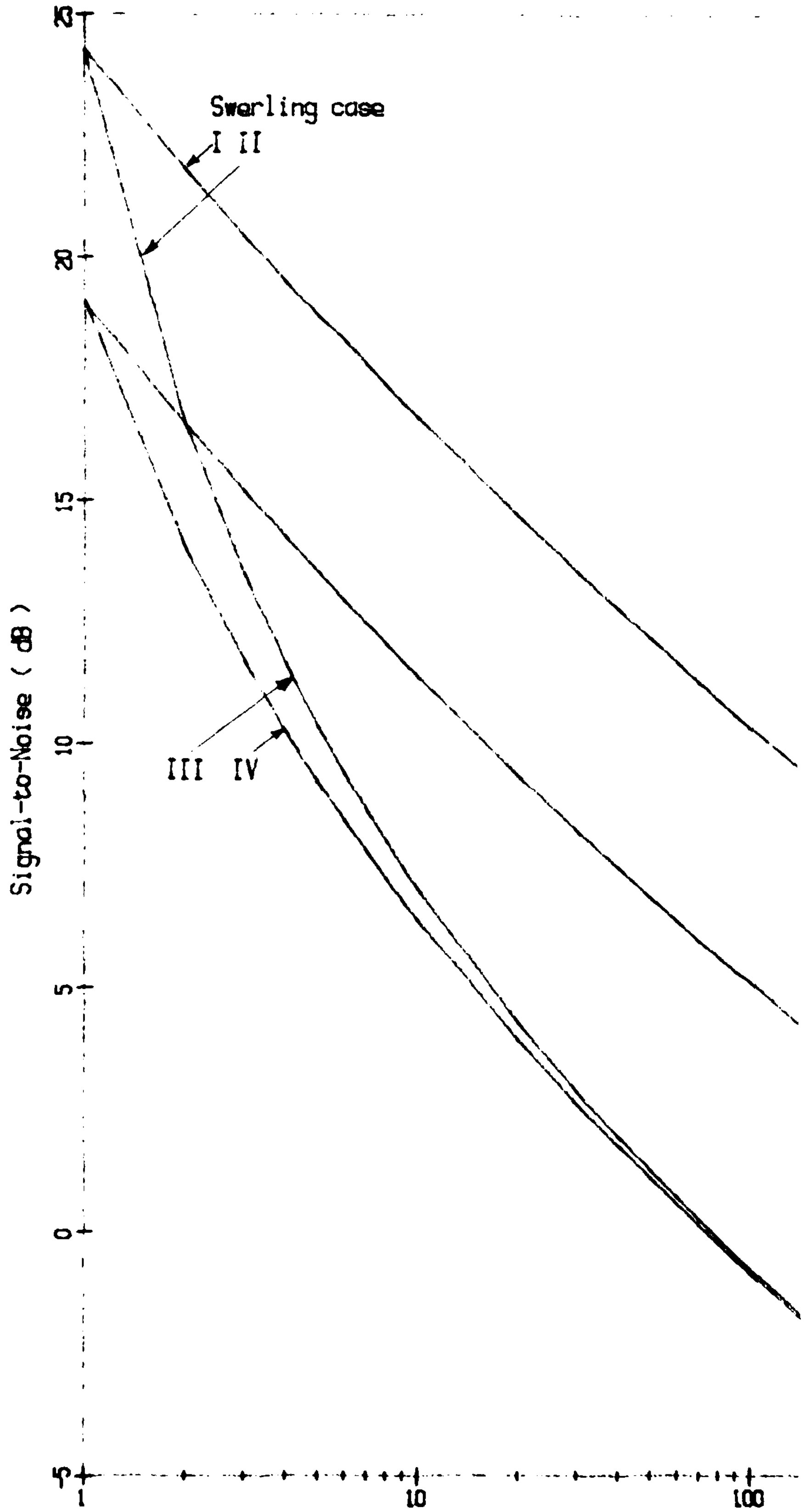

Figure 3. Signal-to-noise required for 95% point prob
PFA = 0.000001. Swerling case I-IV targets.

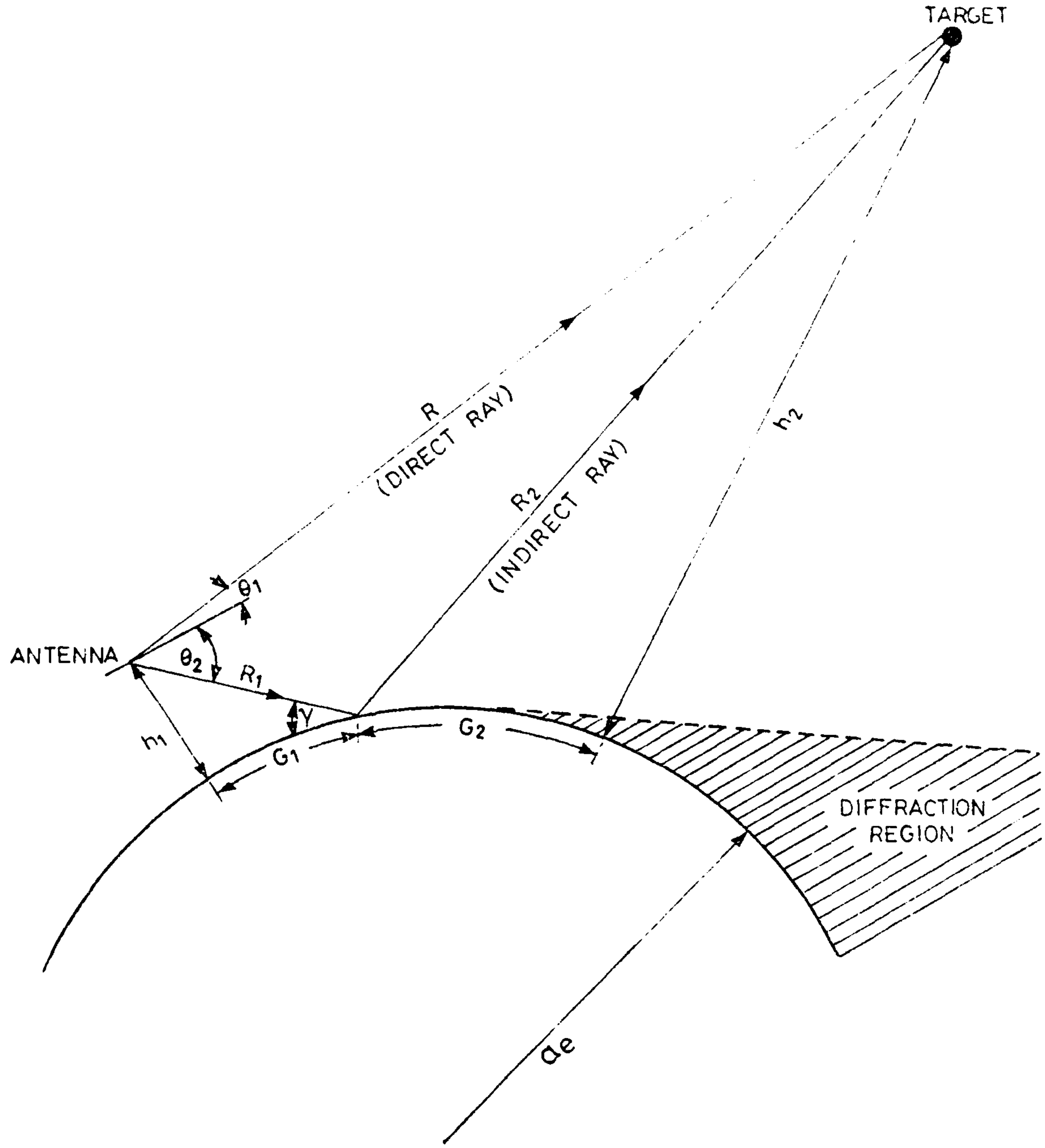

Figure 4. Multipath geometry with symbols as used in text.

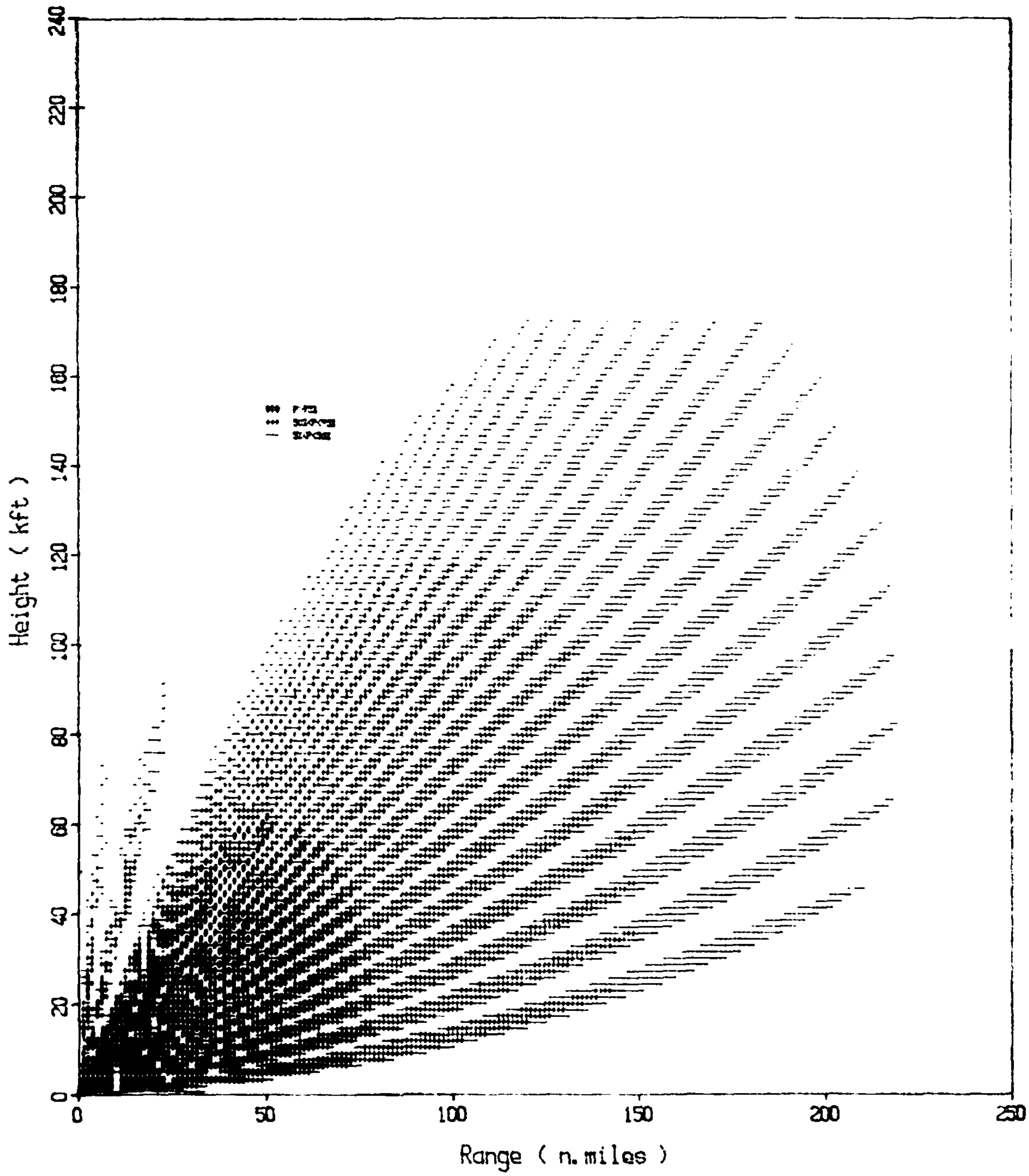

Figure 5. Vertical coverage diagram for UHF radar.
Sea state : 0
Number of pulses integrated : 75
Target : 1 m^2, Swerling case I
Grey scales : 4

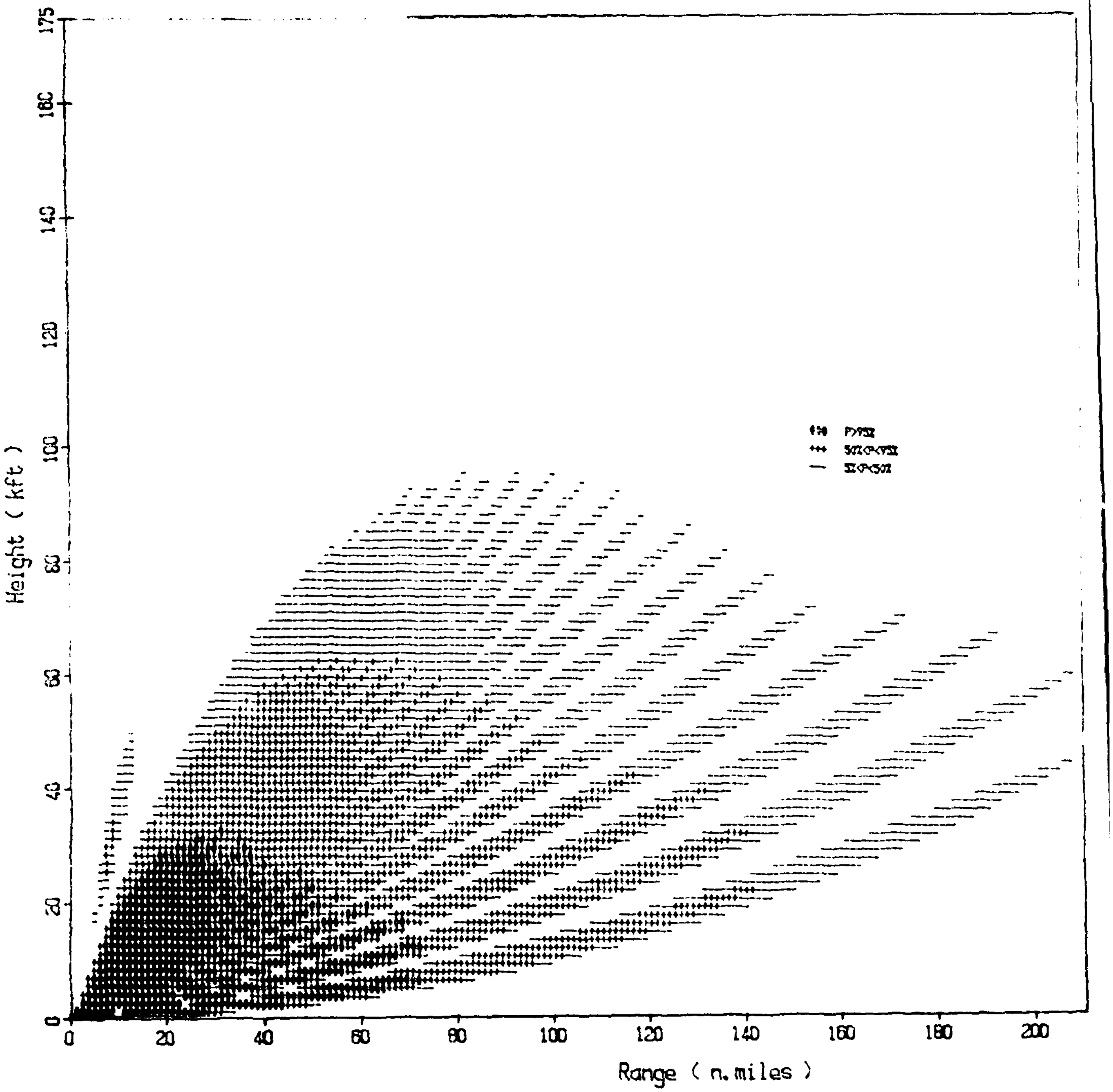

Figure 6. Vertical coverage diagram for UHF radar.
Sea state : 6
Number of pulses integrated : 75
Target : 1 m^2, Swerling case I
Grey scales : 4

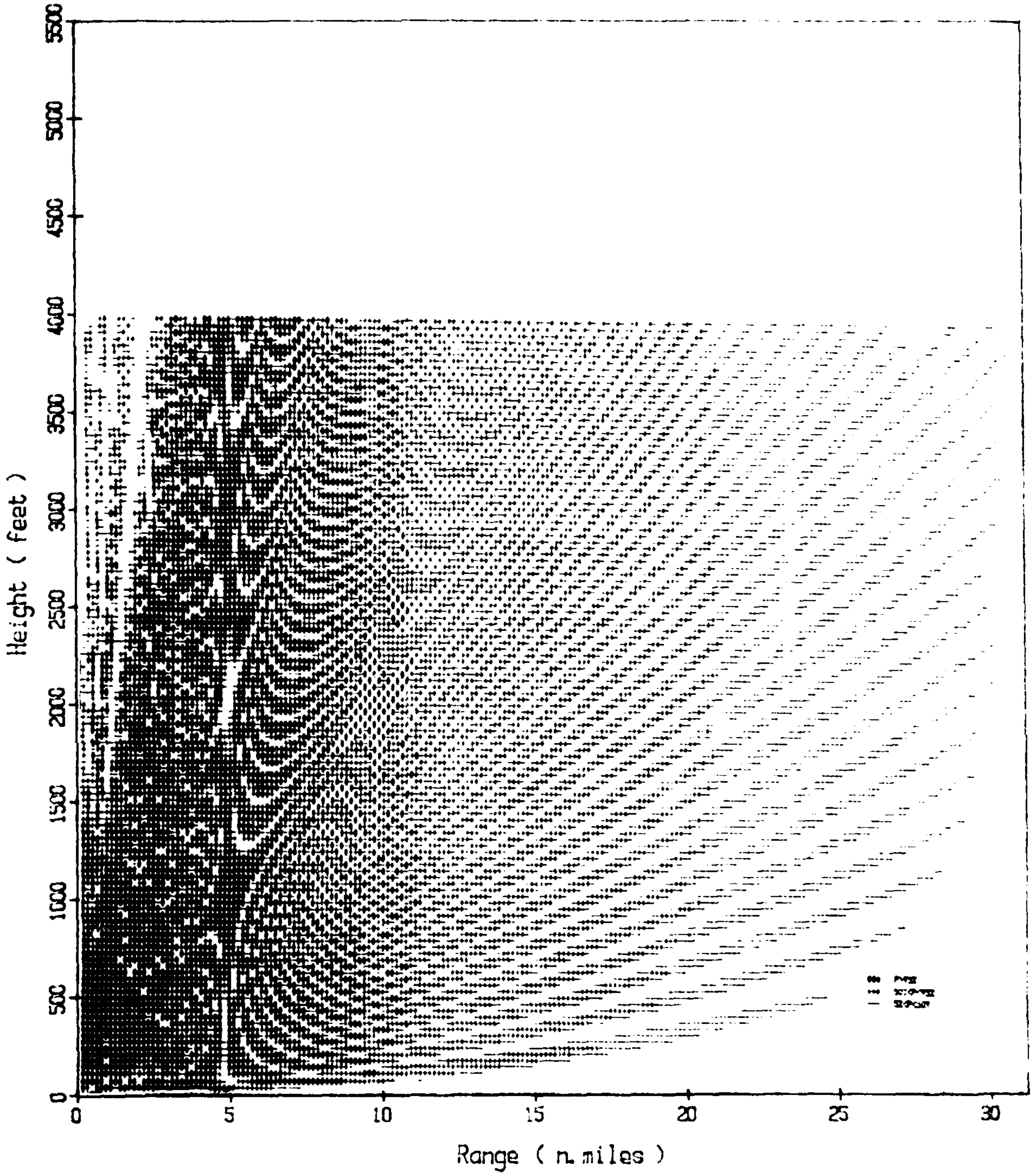

Figure 7. Vertical coverage diagram for G-band radar.
Sea state : 0
Number of pulses integrated : 5
Target : 1 m^2, Swerling case I
Grey scales : 4

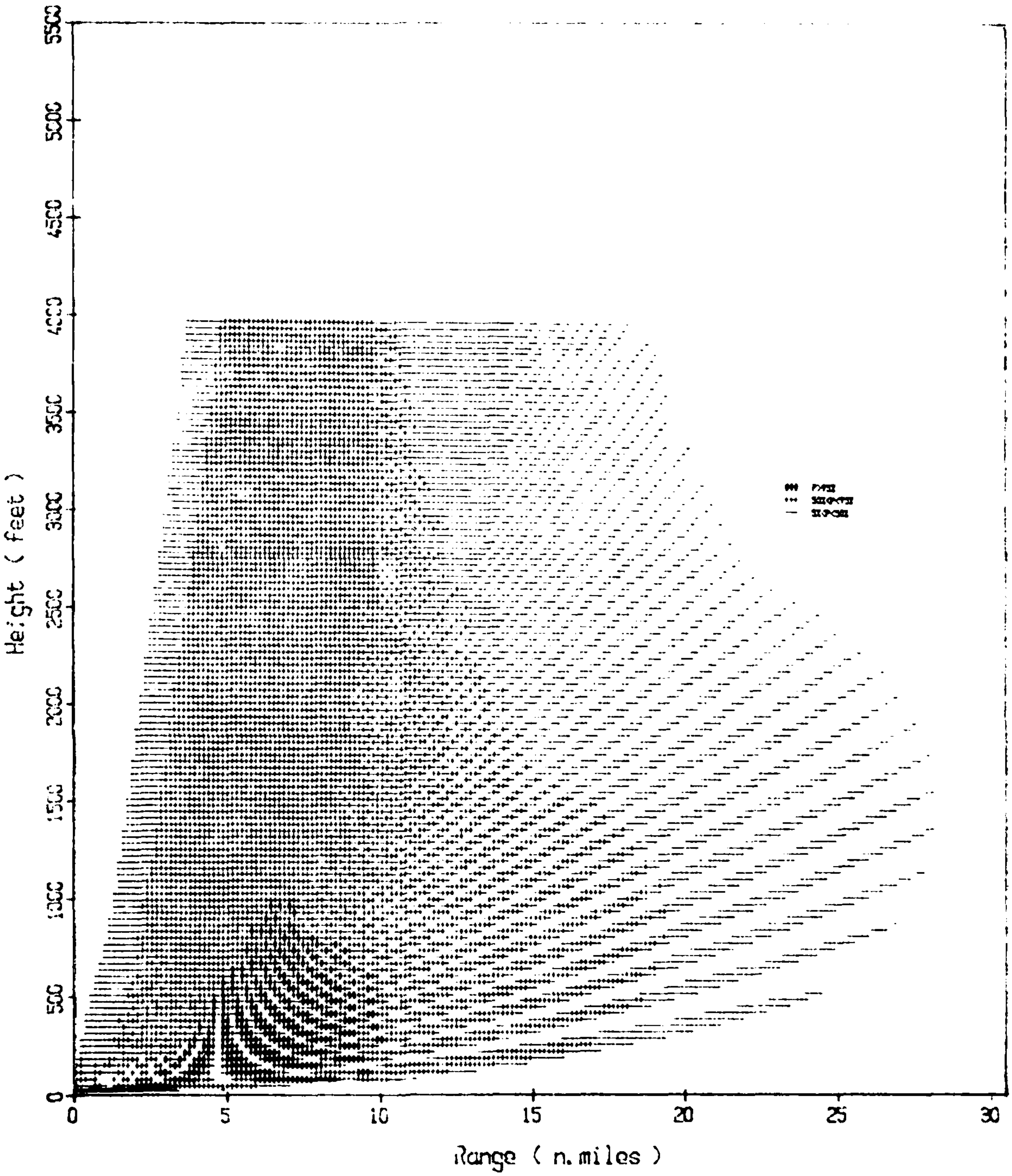

Figure 8. Vertical coverage diagram for S-band radar.
Sea state : 3
Number of pulses integrated : 5
Target : 1 m^2. Swerling case 1
Grey scales : 4

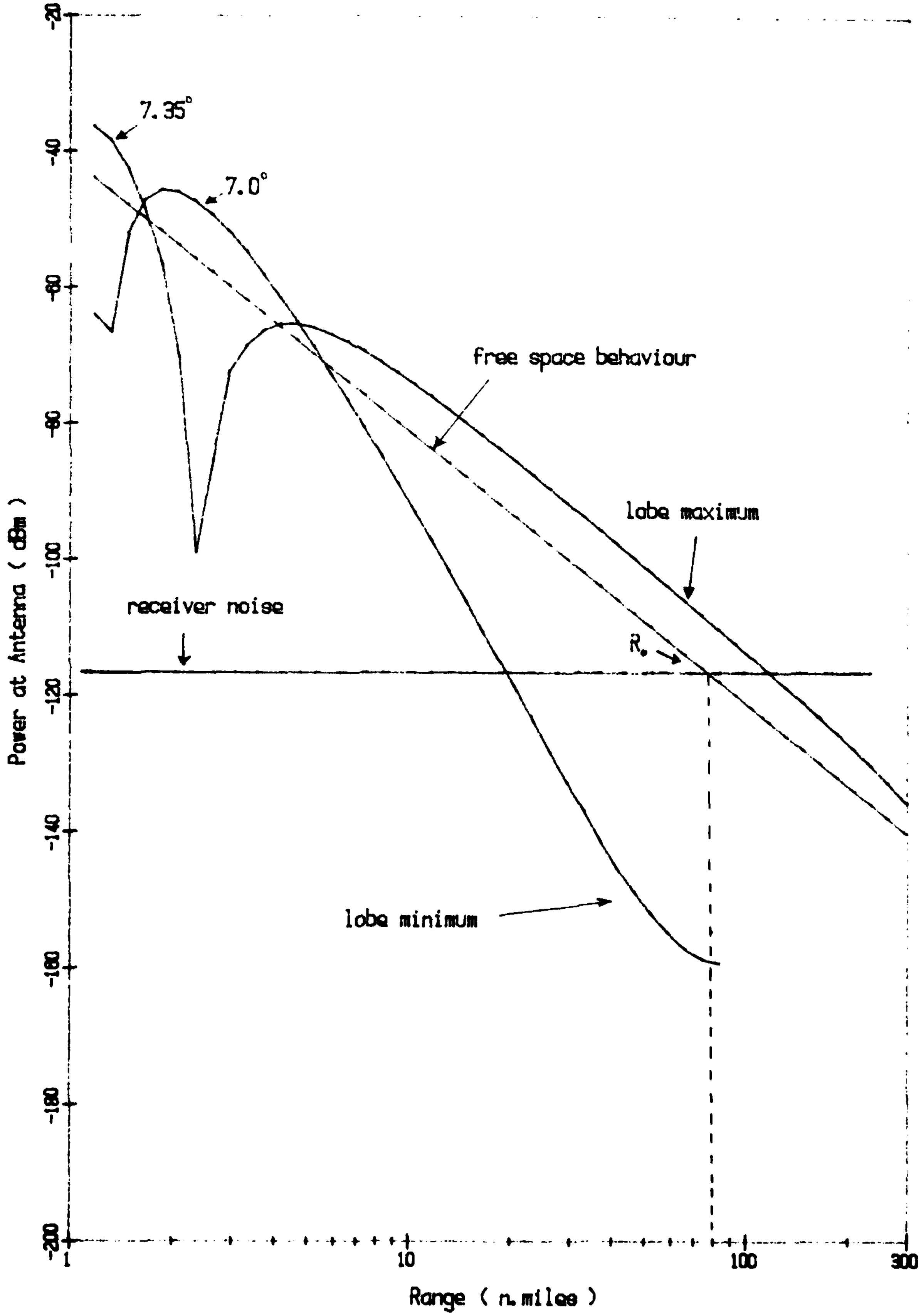

Figure 9. Signal returns for UHF radar at constant elevation angle of 7.0 and 7.35 degrees. Sea state 0.

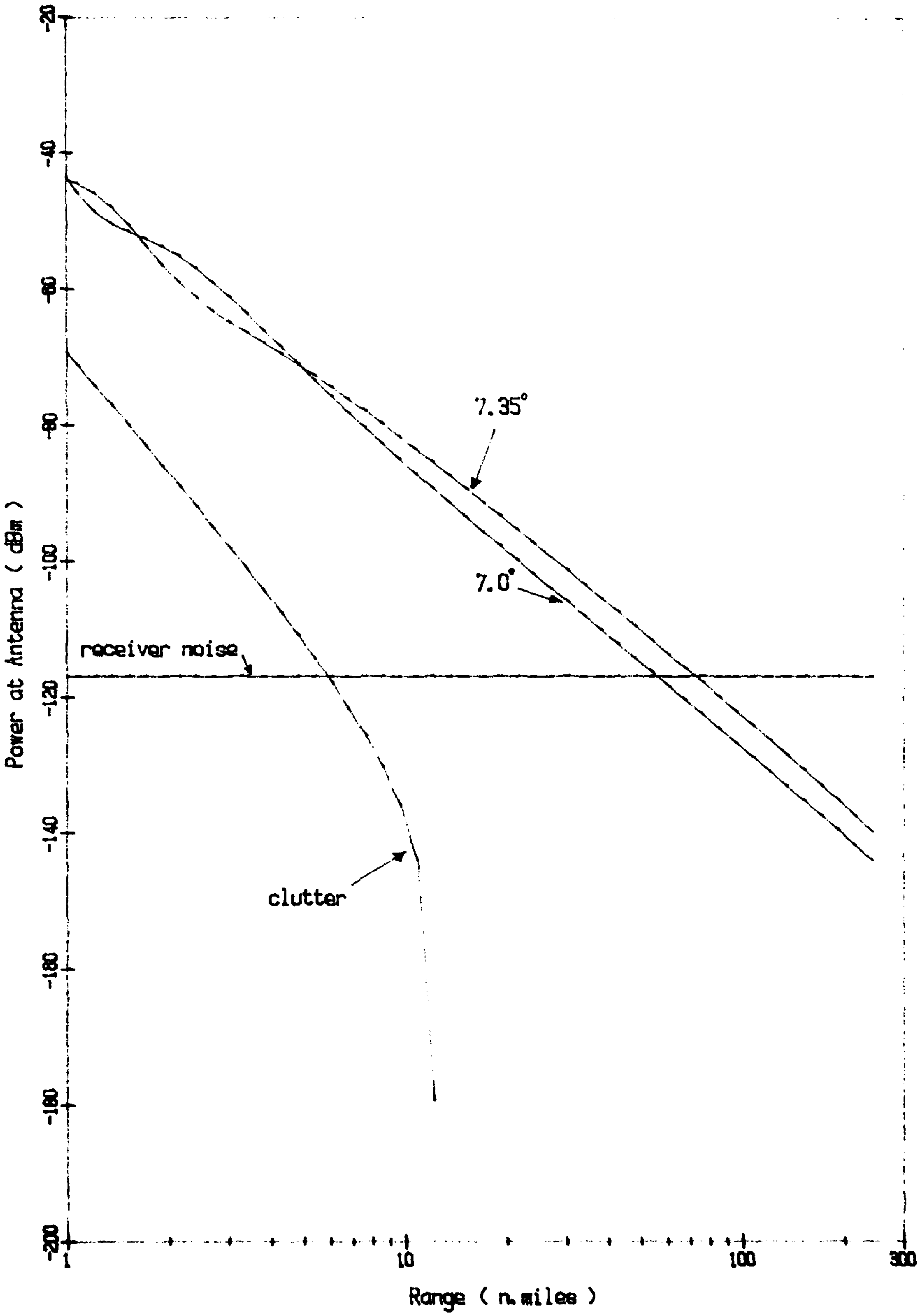

Figure 10. Signal returns for UHF radar at constant elevation angle of 7.0 and 7.35 degrees. Sea state 6.

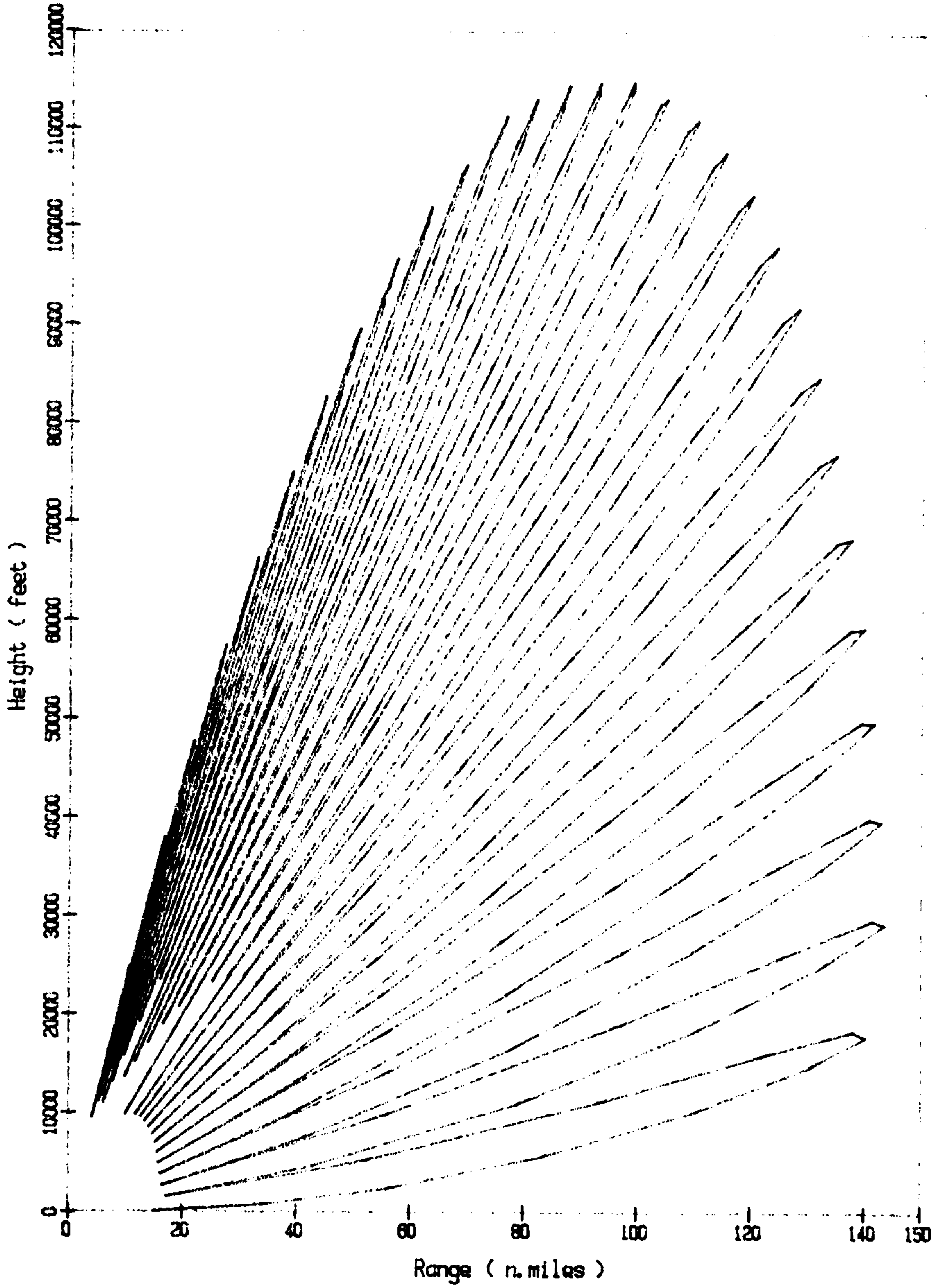

Figure 11. Contour VCD for UHF radar.
Sea state : 0
Signal-to-noise : 0 dB (± 0.25)
Algorithm : Iterative

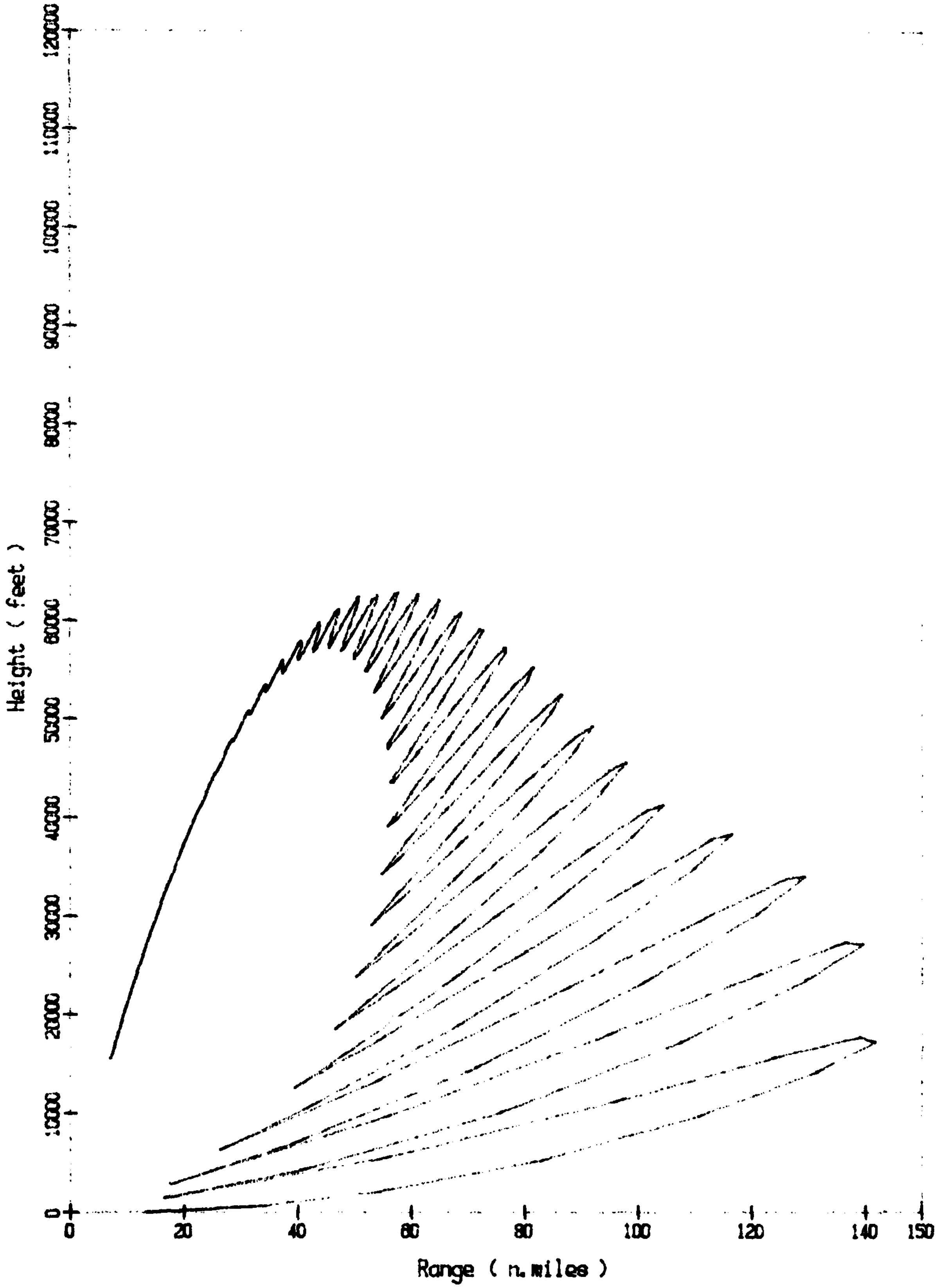

Figure 12. Contour VCD for UHF radar.
Sea state : 6
Signal-to-noise : 0 dB (± 0.25)
Algorithm : Iterative

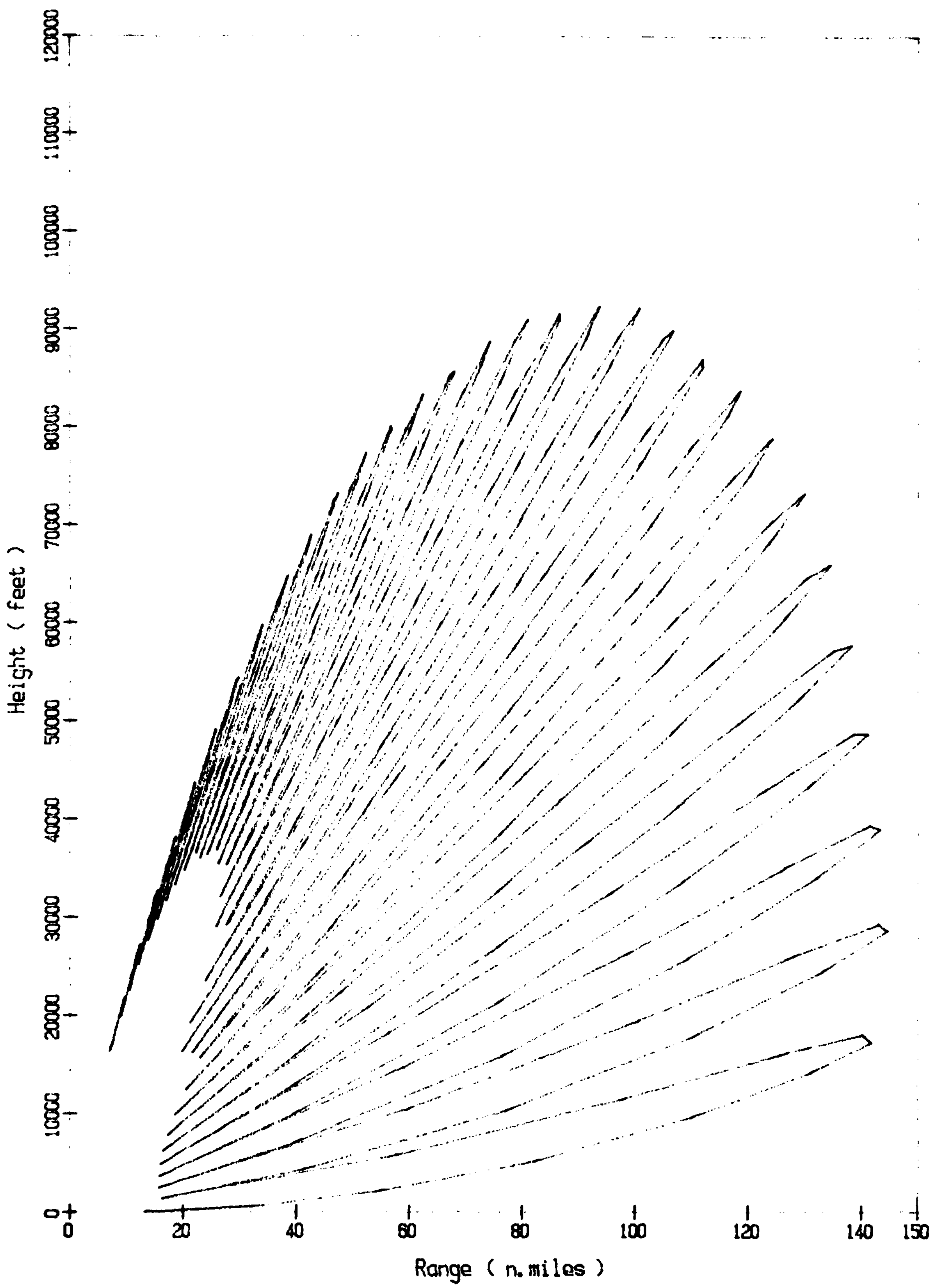

Figure 13. Contour VCD for UHF radar.
Sea state : 3
Signal-to-noise : 0 dB (± 0.25)
Algorithm : Iterative

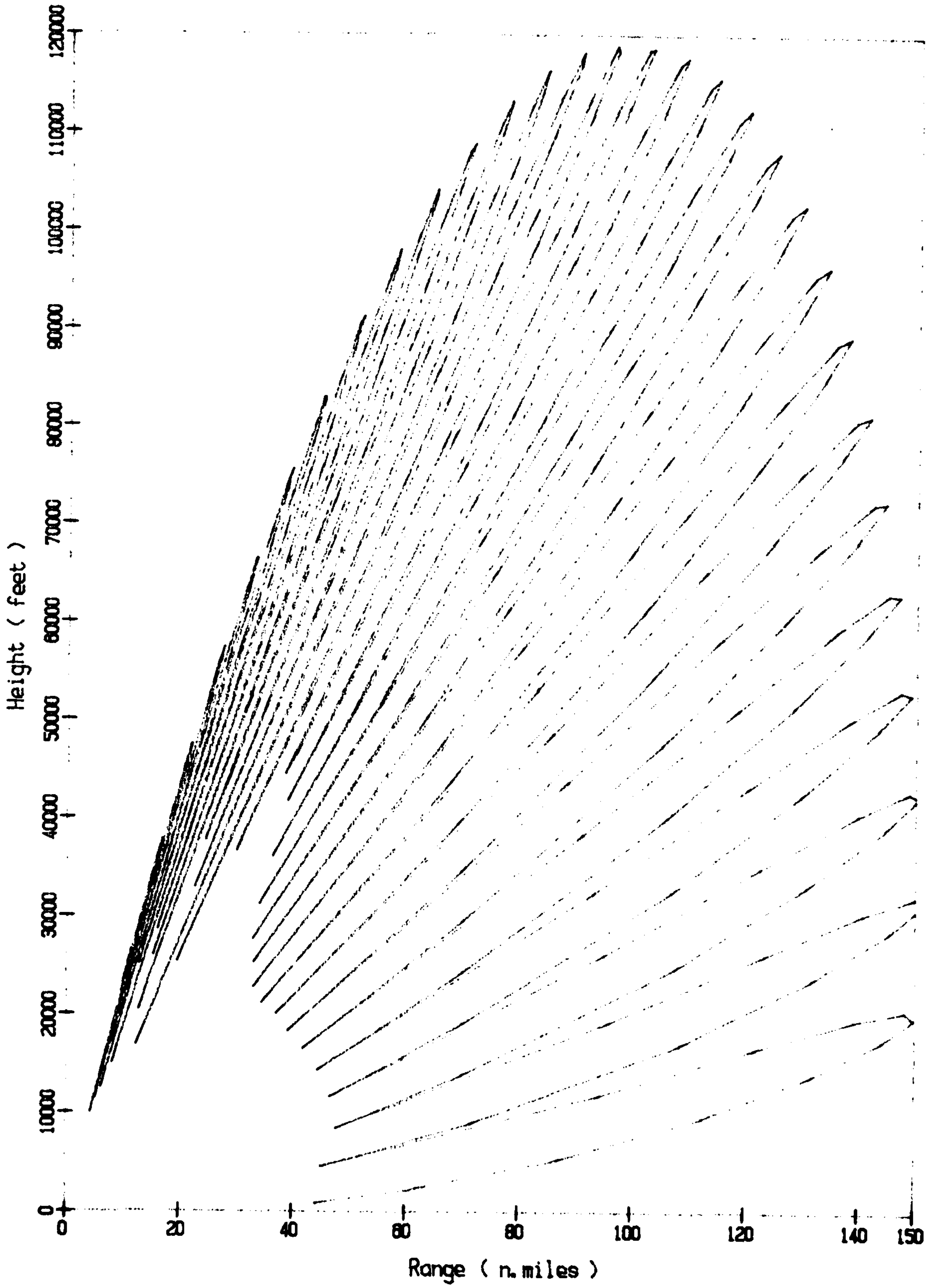

Figure 14. Contour VCD for UHF radar.
Sea state : 0
Signal-to-noise : 0 dB
Algorithm : Scaling

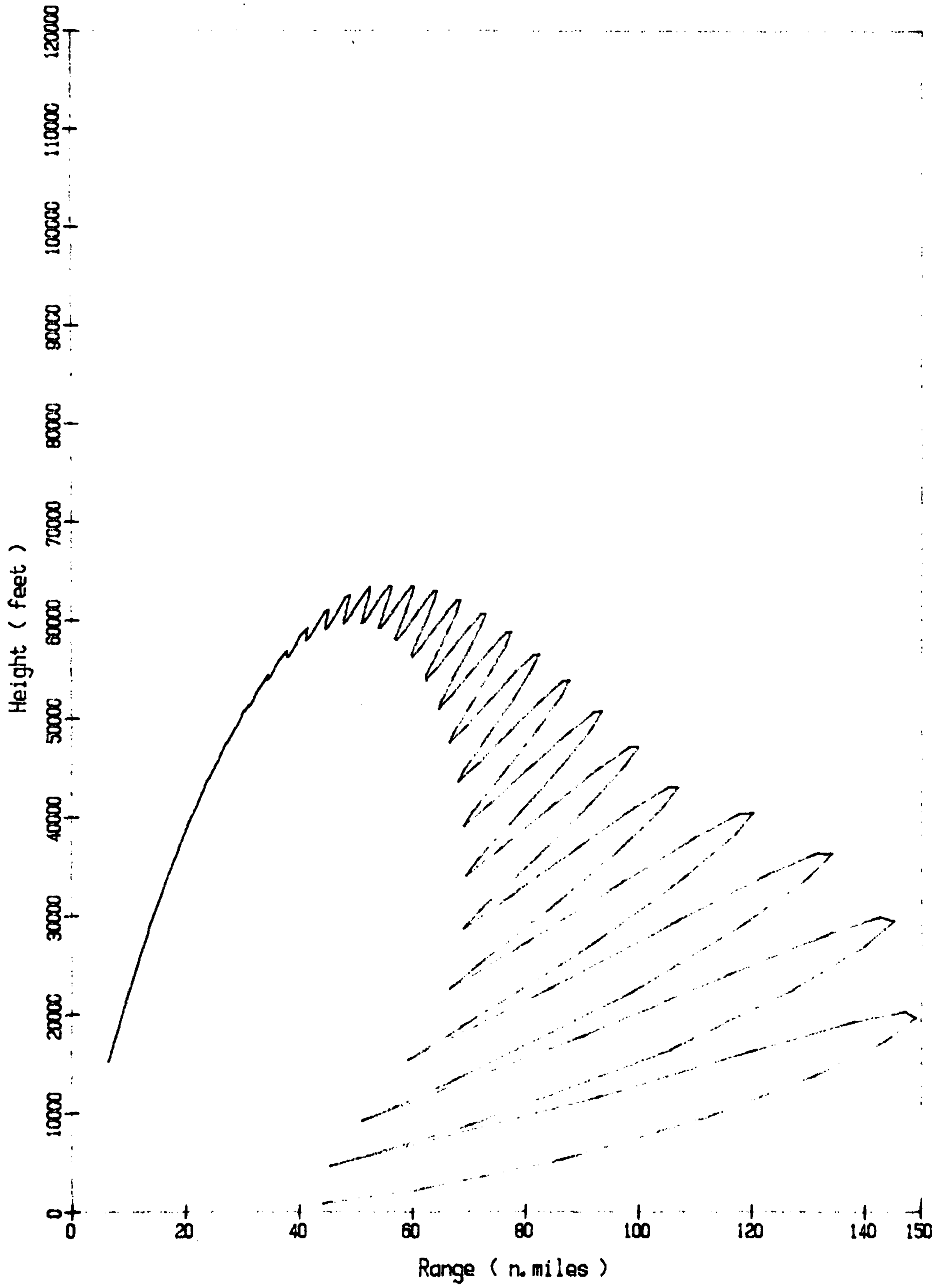

Figure 15. Contour VCD for UHF radar.
Sea state : 6
Signal-to-noise : 0 dB
Algorithm : Scaling

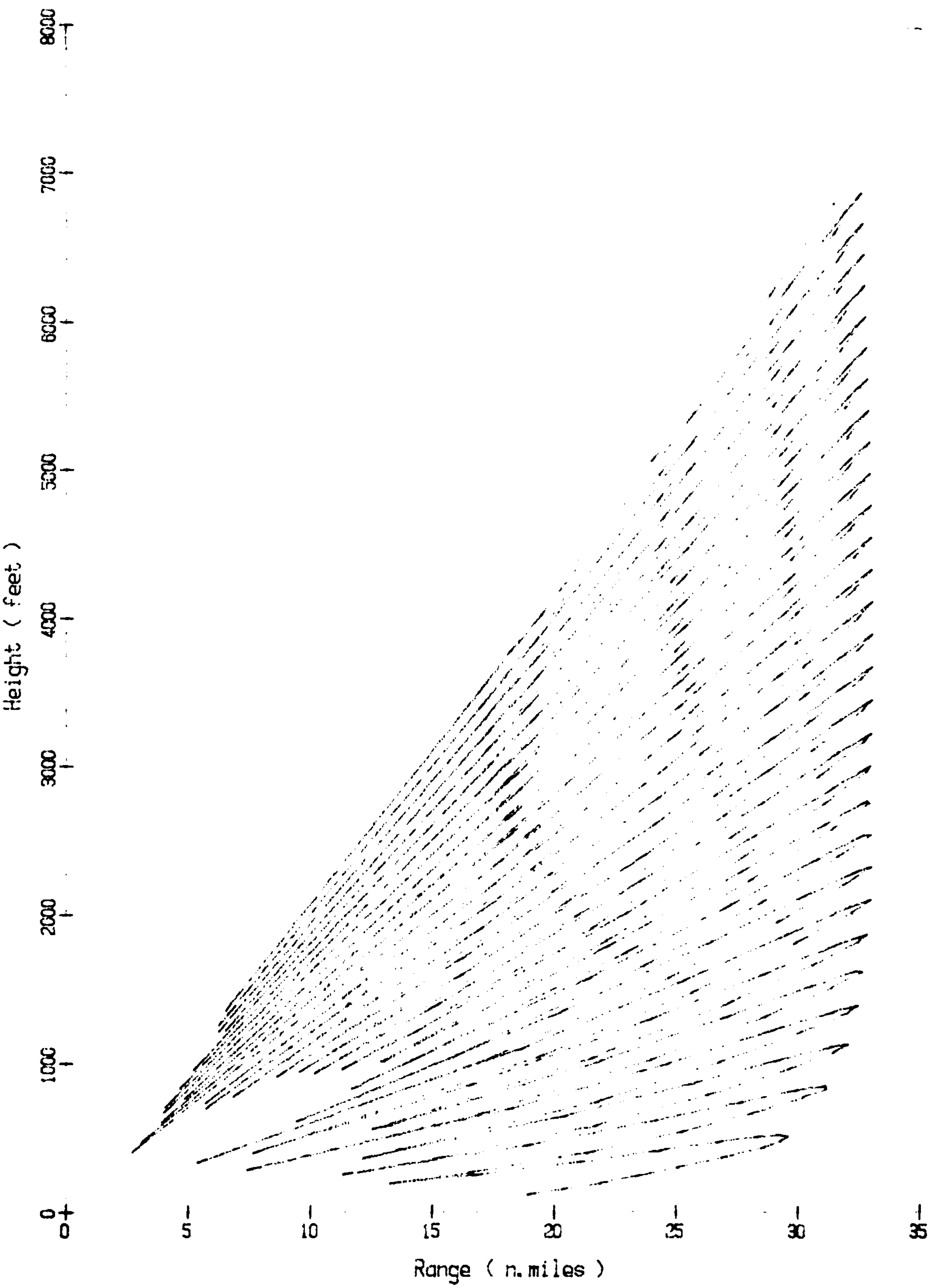

Figure 16. Contour VCD for G-band radar (low angle coverage only).
Sea state : 0
Signal-to-noise : 0 dB
Algorithm : Scaling

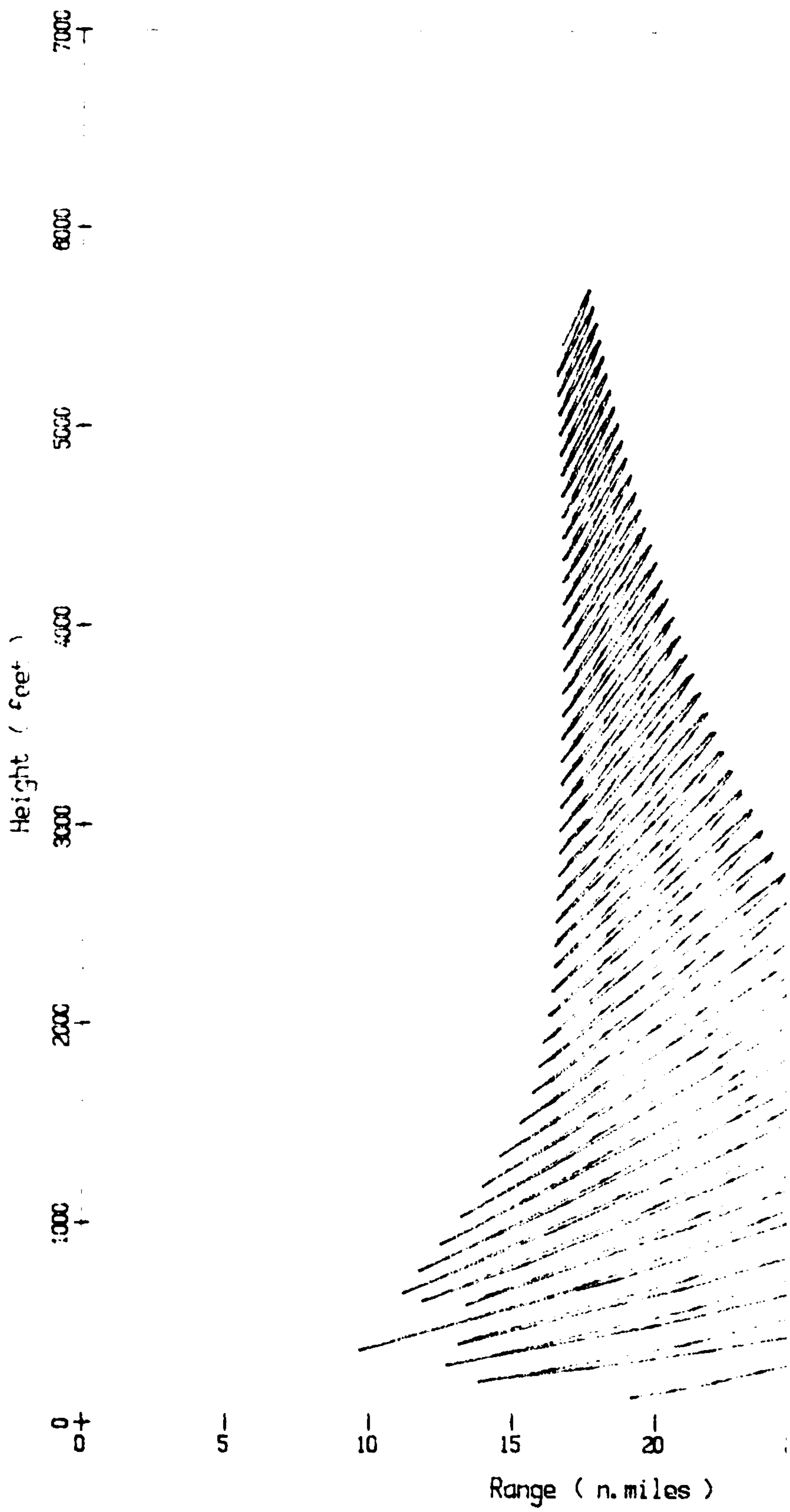

Figure 17. Contour VCD for G-band radar (low angle c
Sea state : 3
Signal-to-noise : 0 dB
Algorithm : Scaling

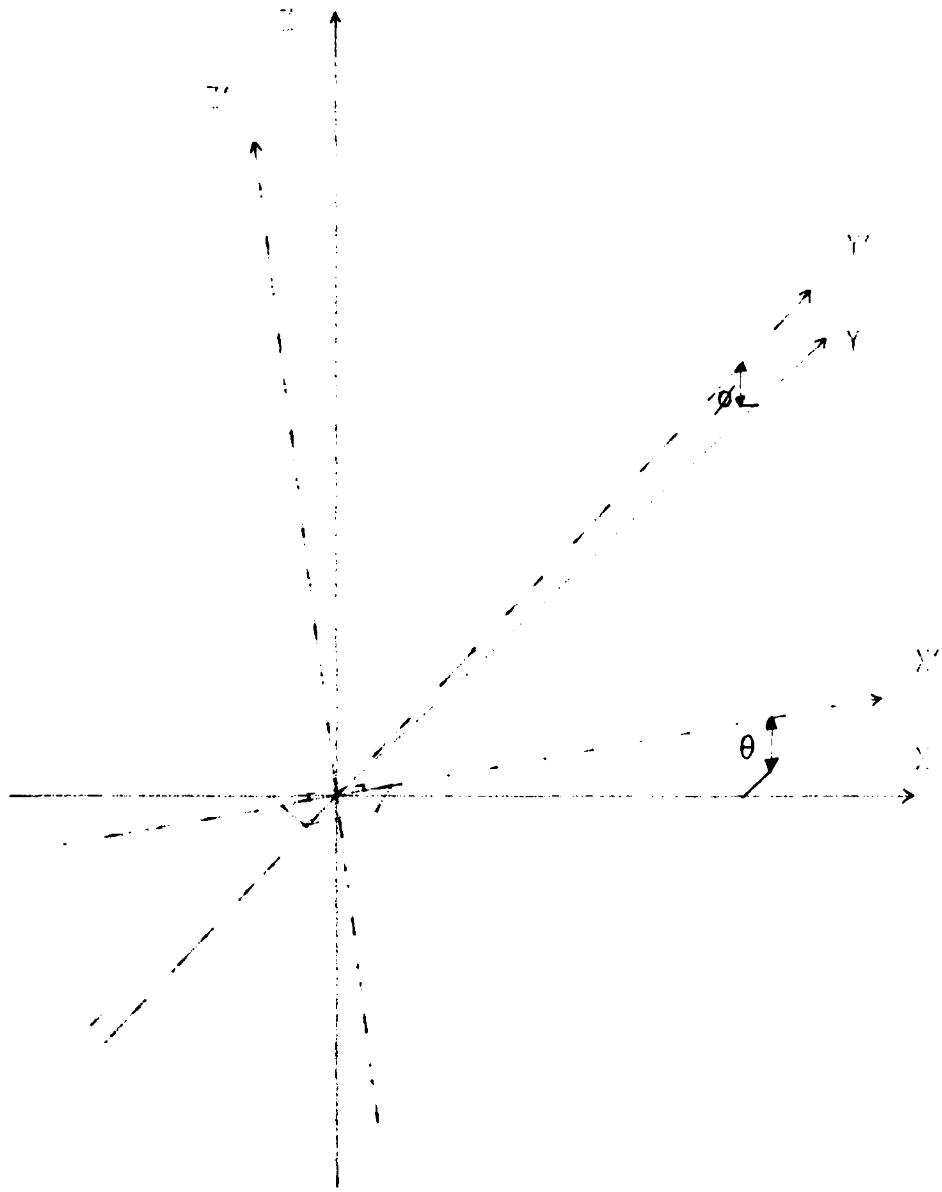

Figure 18. Reference axis systems for discussion of ship motion.

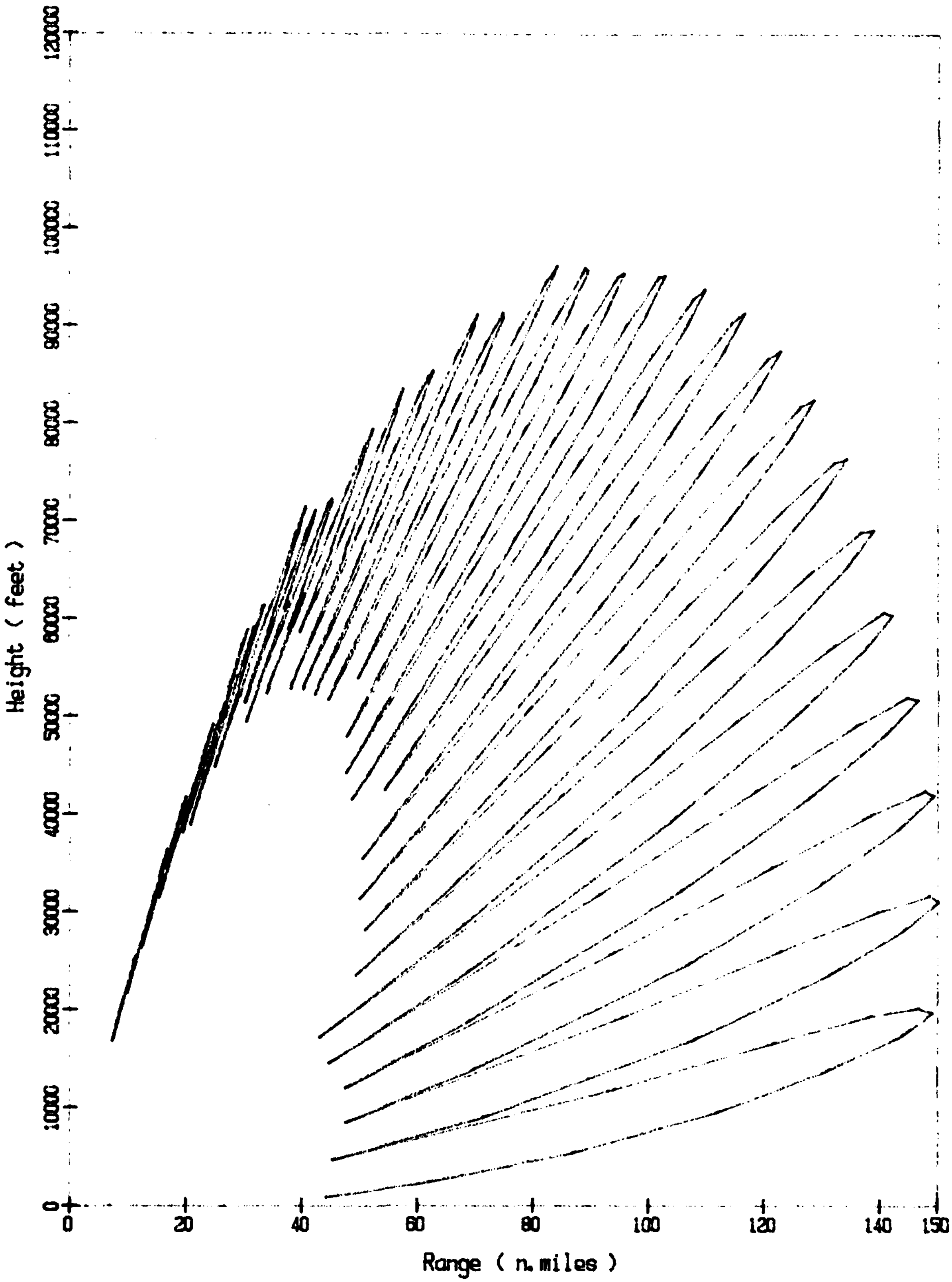

Figure 19. Simulation of the effect of varying antenna tilt for UHF radar
Sea state : 3
Signal-to-noise : 0 dB
Antenna tilt : Random between -10% and + 10% of vert beamwidth
Algorithm : Scaling

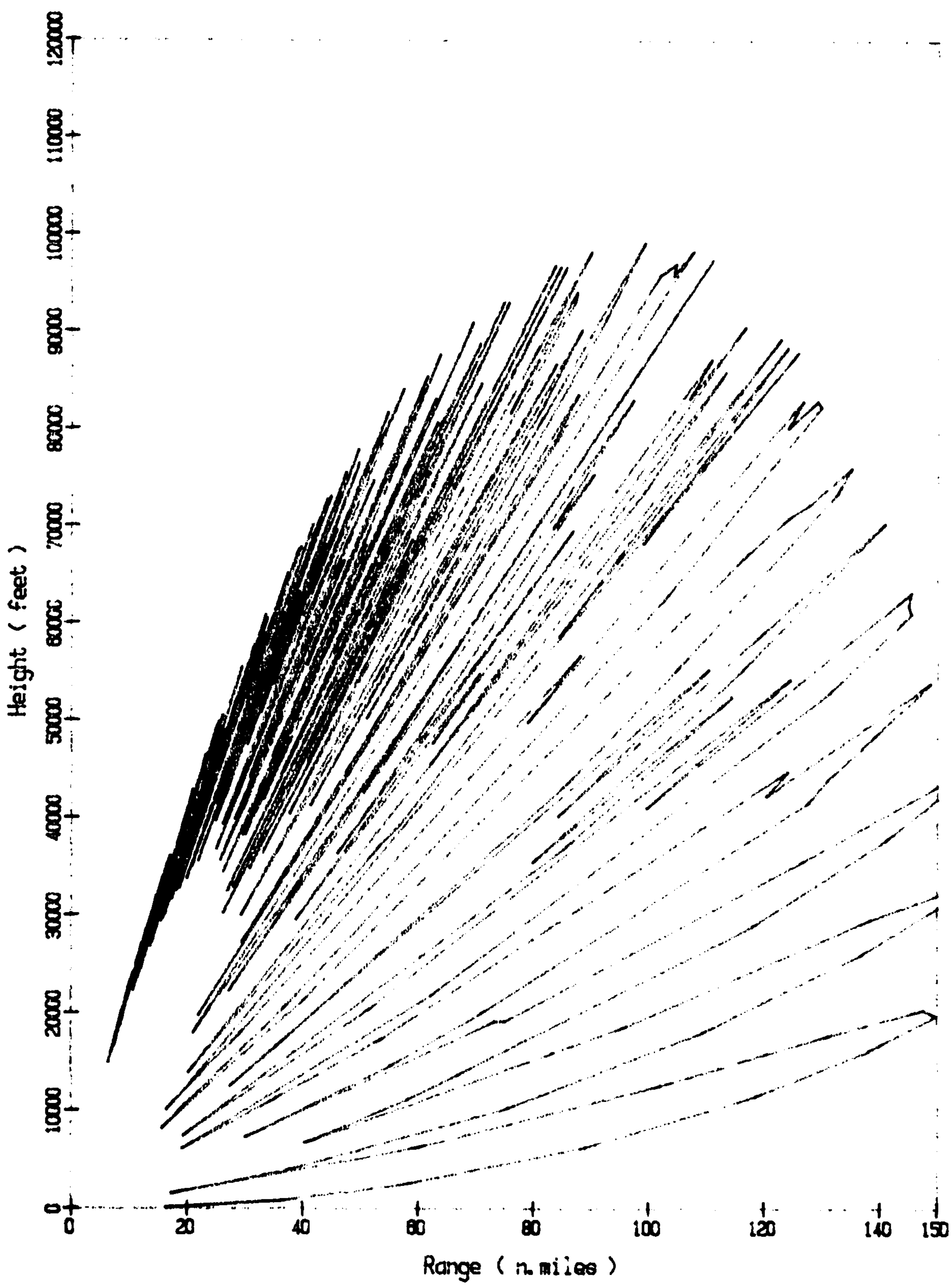

Figure 20. Simulation of effect of varying antenna height for UHF radar
Sea state : 3
Signal-to-noise : 0 dB
Antenna height fluctuation : ± 2.5% of nominal height

DISTRIBUTION

	COPY NO.
Chief Defence Scientist	1
Deputy Chief Defence Scientist	2
CERPAS	3
SSPA	4
JIO (DSTI)	5
RANRL Library master copy	6
Counsellor, Defence Science, Washington	7
Defence Science Rep. London	8
Librarian Technical Reports Centre, Defence Central Library, Campbell Park	9
OIC Document Exchange Centre DISB	10 - 27
Flag Officer Commanding H.M. Australian Fleet	28
Director General, Naval Operational Requirements	29
Director of Tactics, AIO and Navigation	30
Director of Operational Analysis - Navy	31
Director of Surface and Air Weapons - Navy	32
Director of Electronic Warfare - Navy	33
Director of Radar Projects - Air Force	34
Director of Operational Analysis - Air Force	35
Director of Naval Aviation Policy	36
Director, Combat Data System Centre	37
Naval Scientific Adviser	38
Air Force Scientific Adviser	39
Officer-in-Charge RAN Trials and Assessing Unit	40
Director, RAN Tactical School	41
Joint Directors, Australian Joint Anti-Submarine School	42
Senior Librarian, Defence Research Centre Salisbury	43
Senior Librarian, Aeronautical Research Laboratories	44
Librarian H Block, Victoria Barracks, Melbourne	45
Dr M. R. Battaglia	46
Lt Cdr P. Williams, RAN	47
Dr J. L. Whitrow , Electronics Research Laboratory	48
RANRL Library	49 - 53

DOCUMENT CONTROL DATA SHEET

1. a. A.R. No. 003-419	1.b. Establishment No. RANRL Tech Note (External) 1/84	2. Document Date May 1984	3. Task No A3/83
4. Title The Calculation of the Radar Vertical Coverage Diagram		5. Security a. document UNCLAS b. title UNCLAS c. abstract UNCLAS	6. No Pages 45 7. No Refs 8
8. Author(s) BATTAGLIA, M.R.		9. Downgrading Instructions N/A	
10. Corporate Author and Address RAN Research Laboratory P.O. Box 706, Darlinghurst. N.S.W. 2010		11. Authority (as appropriate) a. Sponsor b. Security c. Downgrading d. Approval a. NAV b. HORD c. N/A (unclass) d. M.D. Frost, Director RANRL	
12. Secondary Distribution (of this document) Approved for Public Release			
13. a. This document may be ANNOUNCED in catalogues and awareness services available to : No limitations			
13. b. Citation for other purposes (ie casual announcement) may be as for 13a.			
14. Descriptors Radar, model, multipath, clutter, attenuation, backscatter, probability of detection		15. COSATI Group 17090	

16. Abstract

Algorithms are described for the calculation and plotting of radar vertical coverage diagrams. Two contour VCD algorithms are presented, with a brief discussion on the problem of numerical stability, and the effects of ship motion and frequency agility.

Figure 9. Signal returns for UHF radar at constant elevation angle of 7.0 and 7.35 degrees. Sea state 0.

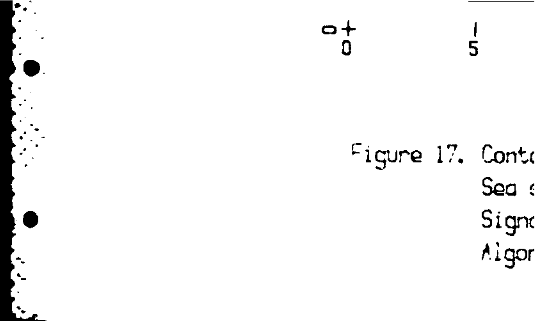

Figure 17. Conto
Sea s
Signa
Algor